Electronic Supplementary Material (ESI) for New Journal of Chemistry.


**Supporting Information**

For

# Highly Selective Solvent Free Catalysis of $CO_2$ and $CS_2$ Fixation Under Mild Condition Using Electronically Varied Zinc Complexes

Souvik Barman[a], Jayanta Bag[a], Dhiraj Das[a, b], and Kuntal Pal*[a]

Department of Chemistry, University of Calcutta, 92 APC Road, Kolkata 700 009, India

## Contents

Figure S1: $^1$H NMR Spectrum of $H_2L^H$ in DMSO- $d_6$. 5
Figure S2: $^{13}$C NMR Spectrum of $H_2L^H$ in DMSO- $d_6$. 6
Figure S3: $^1$H NMR Spectrum of $H_2L^{OMe}$ in DMSO- $d_6$. 6
Figure S4: $^{13}$C NMR Spectrum of $H_2L^{OMe}$ in DMSO- $d_6$. 7
Figure S5: $^1$H NMR Spectrum of $H_2L^{NO2}$ in DMSO- $d_6$. 7
Figure S6: $^{13}$C NMR Spectrum of $H_2L^{NO2}$ in DMSO- $d_6$ 8
Figure S7: $^1$H NMR Spectrum of [Zn($L^H$)] in DMSO- $d_6$. 8
Figure S8: $^{13}$C NMR Spectrum of [Zn($L^H$)] in DMSO- $d_6$. 9
Figure S9: $^1$H NMR Spectrum of [Zn($L^{OMe}$)] in DMSO- $d_6$. 9
Figure S10: $^{13}$C NMR Spectrum of [Zn($L^{OMe}$)] in DMSO- $d_6$. 10
Figure S11: $^1$H NMR Spectrum of [Zn($L^{NO2}$)] in DMSO- $d_6$. 10
Figure S12: $^{13}$C NMR Spectrum of [Zn($L^{NO2}$)] in DMSO- $d_6$. 11
Figure S13: $^1$H NMR Spectrum of [Zn($L^H$)(DMF)] in DMSO- $d_6$. 11
Figure S14: $^{13}$C NMR Spectrum of [Zn($L^H$)(DMF)] in DMSO- $d_6$. 12
Figure S15: $^1$H NMR Spectrum of [Zn($L^{NO2}$)(DMF)] in DMSO- $d_6$. 12
Figure S16: $^{13}$C NMR Spectrum of [Zn($L^{NO2}$)(DMF)] in DMSO- $d_6$. 13
Figure S17: $^1$H NMR Spectrum of [Zn($L^H$)Br]($Bu_4N$) in DMSO-$d_6$. 13
Figure S18: $^{13}$C NMR Spectrum of [Zn($L^H$)Br]($Bu_4N$) in DMSO-$d_6$. 13
Figure S19: $^1$H NMR Spectrum of [Zn($L^{OMe}$)Br]($Bu_4N$) in DMSO-$d_6$. 14
Figure S20: $^{13}$C NMR Spectrum of [Zn($L^{OMe}$)Br]($Bu_4N$) in DMSO-$d_6$. 14
Figure S21: $^1$H NMR Spectrum of [Zn($L^{NO2}$)Br]($Bu_4N$) in DMSO-$d_6$. 15
Figure S22: $^{13}$C NMR Spectrum of [Zn($L^{NO2}$)Br]($Bu_4N$) in DMSO-$d_6$. 15
Figure S23: ESI-MS spectrum of $H_2L^H$ 16

Figure S24: ESI-MS spectrum of $H_2L^{OMe}$. 17
Figure S25: ESI-MS spectrum of $H_2L^{NO2}$. 17
Figure S26: ESI-MS Spectrum of [Zn($L^{H}$)]. 18
Figure S27: ESI-MS Spectrum of [Zn($L^{OMe}$)]. 18
Figure S28: ESI-MS Spectrum of [Zn($L^{NO2}$)]. 19
Figure S29: ESI-MS Spectrum of [Zn($L^{H}$)(DMF)]. 20
Figure S30: ESI-MS Spectrum of [Zn($L^{NO2}$)(DMF)]. 21
Figure S31: ESI-MS Spectrum of [Zn($L^{H}$)Br]($Bu_4N$). 22
Figure S32: ESI-MS Spectrum of [Zn($L^{OMe}$)Br]($Bu_4N$). 22
Figure S33: ESI-MS Spectrum of [Zn($L^{NO2}$)Br]($Bu_4N$). 23
Figure S34: FT-IR spectrum of $H_2L^{H}$. 24
Figure S35: FT-IR spectrum of $H_2L^{OMe}$. 24
Figure S36: FT-IR spectrum of $H_2L^{NO2}$. 25
Figure S37: FT-IR Spectrum of [Zn($L^{H}$)]. 25
Figure S38: FT-IR Spectrum of [Zn($L^{OMe}$)]. 26
Figure S39: FT-IR Spectrum of [Zn($L^{NO2}$)]. 26
Figure S40: FT-IR Spectrum of [Zn($L^{H}$)(DMF)]. 27
Figure S41: FT-IR Spectrum of [Zn($L^{NO2}$)(DMF)]. 27
Figure S42: FT-IR Spectrum of [Zn($L^{H}$)Br]($Bu_4N$). 28
Figure S43: FT-IR Spectrum of [Zn($L^{OMe}$)Br]($Bu_4N$). 28
Figure S44: FT-IR Spectrum of [Zn($L^{NO2}$)Br]($Bu_4N$). 29
Figure S45: Electronic absorption spectra of $H_2L^{H}$ (1 x $10^{-5}$(M) in $CH_3CN$). 29
Figure S46: Electronic absorption spectra of $H_2L^{OMe}$ (5 x $10^{-5(}$M) in $CH_3CN$). 30
Figure S47: Electronic absorption spectra of $H_2L^{NO2}$ (5 x $10^{-5}$(M) in $CH_3CN$). 30
Figure S48: Electronic absorption spectra of [Zn($L^{H}$)] (1 x $10^{-5}$(M) in DMF). 31
Figure S49: Electronic absorption spectra of [Zn($L^{OMe}$)] (1 x $10^{-5}$(M) in DMF). 31
Figure S50: Electronic absorption spectra of [Zn($L^{NO2}$)] (1 x $10^{-5}$(M) in $CH_3CN$). 32
Figure S51: Electronic absorption spectra of [Zn($L^{H}$)(DMF)] (1 x $10^{-5}$(M) in $CH_3CN$). 32
Figure S52: Electronic absorption spectra of [Zn($L^{NO2}$)(DMF)] (1 x $10^{-5}$(M) in DMF). 33
Figure S53: Electronic absorption spectra of [Zn($L^{H}$)Br]($Bu_4N$) (5 x $10^{-5(}$M) in $CH_3CN$). 33
Figure S54: Electronic absorption spectra of [Zn($L^{OMe}$)Br]($Bu_4N$) (1 x $10^{-5(}$M) in $CH_3CN$). 34
Figure S55: Electronic absorption spectra of [Zn($L^{NO2}$)Br]($Bu_4N$) (1 x $10^{-5(}$M) in $CH_3CN$). 34

Figure S56: $^1$H NMR Spectrum in $CDCl_3$ obtained for a reaction mixture taken after 24 hrs ([Zn($L^H$)]: 1 mol%, TBAB: 10 mol%) showing three peaks of styrene carbonate and three peaks associated to styrene oxide starting material (19% conversion) [* indicates Tetrabutyl ammonium bromide (TBAB) peaks]…35

Figure S56a: $^1$H NMR Spectrum in $CDCl_3$ obtained for a reaction mixture taken after 24 hrs (TBAB: 10 mol%) without catalyst showing three peaks of styrene carbonate and three peaks associated to styrene oxide starting material (7% conversion) [* indicates Tetrabutyl ammonium bromide (TBAB) peaks]. ....36

Figure S57: $^1$H NMR Spectrum in $CDCl_3$ obtained for a reaction mixture taken after 24 hrs ([Zn($L^H$)]: 2 mol%, TBAB: 10 mol%) showing three peaks of styrene carbonate and three peaks associated to styrene oxide starting material (23% conversion) [* indicates Tetrabutyl ammonium bromide (TBAB) peaks]…36

Figure S57a: $^1$H NMR Spectrum in $CDCl_3$ obtained for a reaction mixture taken after 24 hrs ([Zn($L^H$)]: 5 mol%, TBAB: 5 mol%) showing three peaks of styrene carbonate and three peaks associated to styrene oxide starting material (33% conversion) [* indicates Tetrabutyl ammonium bromide (TBAB) peaks]…37

Figure S58: $^1$H NMR Spectrum in $CDCl_3$ obtained for a reaction mixture taken after 24 hrs ([Zn($L^H$)]: 5 mol%, TBAB: 10 mol%) showing three peaks of styrene carbonate and three peaks associated to styrene oxide starting material (41% conversion) [* indicates Tetrabutyl ammonium bromide (TBAB) peaks]…38

Figure S59: $^1$H NMR Spectrum in $CDCl_3$ obtained for a reaction mixture taken after 24 hrs ([Zn($L^H$)]: 5 mol%, TBAB: 20 mol%) showing three peaks of styrene carbonate and three peaks associated to styrene oxide starting material (74% conversion) [* indicates Tetrabutyl ammonium bromide (TBAB) peaks]…39

Figure S60: $^1$H NMR Spectrum in $CDCl_3$ obtained for a reaction mixture taken after 48 hrs ([Zn($L^H$)]: 5 mol%, TBAB: 20 mol%) showing three peaks of styrene carbonate (>99% conversion) [* indicates Tetrabutyl ammonium bromide (TBAB) peaks]. ....40

Figure S61: $^1$H NMR Spectrum in $CDCl_3$ obtained for a reaction mixture taken after 24 hrs ([Zn($L^{NO2}$)]: 5 mol%, TBAB: 20 mol%) showing three peaks of styrene carbonate and three peaks associated to styrene oxide starting material (70% conversion) [* indicates Tetrabutyl ammonium bromide (TBAB) peaks]…41

Figure S62: $^1$H NMR Spectrum in $CDCl_3$ obtained for a reaction mixture taken after 24 hrs ([Zn($L^{OMe}$)]: 5 mol%, TBAB: 20 mol%) showing three peaks of styrene carbonate and three peaks associated to styrene oxide starting material (35% conversion) [* indicates Tetrabutyl ammonium bromide (TBAB) peaks]…42

Figure S63: $^1$H NMR Spectrum in $CDCl_3$ obtained for a reaction mixture taken after 24 hrs ([Zn($L^H$)]: 5 mol%, TBAB: 20 mol%) showing product peaks of cyclohexane carbonate (CHC) (>99% conversion) [* indicates Tetrabutyl ammonium bromide (TBAB) peaks]. ....43

Figure S64: $^1$H NMR Spectrum in $CDCl_3$ obtained for a reaction mixture taken after 24 hrs ([Zn($L^{NO2}$)]: 5 mol%, TBAB: 20 mol%) showing product peaks of cyclohexane carbonate (CHC) (>99% conversion) [* indicates Tetrabutyl ammonium bromide (TBAB) peaks]. ....44

Figure S65: $^1$H NMR Spectrum in $CDCl_3$ obtained for a reaction mixture taken after 24 hrs ([Zn($L^{OMe}$)]: 5 mol%, TBAB: 20 mol%) showing product peaks of cyclohexane carbonate (CHC) (>99% conversion) [* indicates Tetrabutyl ammonium bromide (TBAB) peaks]. ....44

Figure S66: $^1$H NMR in $CDCl_3$ obtained for a reaction mixture taken after 24 hrs ([Zn($L^H$)]: 5 mol%, TBAB: 20 mol%, $CS_2$: 0.3 mL) showing three different products and three peaks associated to styrene oxide starting material [* indicates Tetrabutyl ammonium bromide (TBAB) peaks]. ....45

Figure S67: $^{1}H$ NMR in $CDCl_3$ obtained for a reaction mixture taken after 48 hrs ([Zn($L^{H}$)]: 5 mol%, TBAB: 20 mol%, $CS_2$: 0.3 mL) showing two different products [* indicates Tetrabutyl ammonium bromide (TBAB) peaks]. ..... 46

Figure S68: $^{1}H$ NMR in $CDCl_3$ obtained for a reaction mixture taken after 24 hrs ([Zn($L^{NO2}$)]: 5 mol%, TBAB: 20 mol%, $CS_2$: 0.3 mL) showing three different products and three peaks associated to styrene oxide starting material [* indicates Tetrabutyl ammonium bromide (TBAB) peaks]. ..... 47

Figure S69: $^{1}H$ NMR in $CDCl_3$ obtained for a reaction mixture taken after 48 hrs ([Zn($L^{NO2}$)]: 5 mol%, TBAB: 20 mol%, $CS_2$: 0.3 mL) showing three different products [* indicates Tetrabutyl ammonium bromide (TBAB) peaks]. ..... 48

Figure S70: $^{1}H$ NMR in $CDCl_3$ obtained for a reaction mixture taken after 24 hrs ([Zn($L^{OMe}$)]: 5 mol%, TBAB: 20 mol%, $CS_2$: 0.3 mL) showing three different products and three peaks associated to styrene oxide starting material [* indicates Tetrabutyl ammonium bromide (TBAB) peaks]. ..... 48

Figure S71: $^{1}H$ NMR in $CDCl_3$ obtained for a reaction mixture taken after 48 hrs ([Zn($L^{OMe}$)]: 5 mol%, TBAB: 20 mol%, $CS_2$: 0.3 mL) showing two different products and three peaks associated to styrene oxide starting material [* indicates Tetrabutyl ammonium bromide (TBAB) peaks]. ..... 49

Figure S72: $^{1}H$ NMR spectrum of 4-Phenyl-1,3-dithiolane-2-thione in $CDCl_3$. ..... 50

Figure S73: $^{13}C$ NMR spectrum of 4-Phenyl-1,3-dithiolane-2-thione in $CDCl_3$. ..... 50

Figure S74: $^{1}H$ NMR spectrum of 5-phenyl-1,3-oxathiolane-2-thione and 4-phenyl-1,3-oxathiolane-2-thione in $CDCl_3$. ..... 51

Figure S75: $^{13}C$ NMR spectrum of 5-phenyl-1,3-oxathiolane-2-thione and 4-phenyl-1,3-oxathiolane-2-thione in $CDCl_3$. ..... 51

Figure S76: Carbonyl region of $^{13}C$ NMR spectrum of cyclohexane carbonate synthesized using Zn-$1^{H}$ (Table 5, Reaction 2). ..... 51

Figure S77: Comparison between the $^{1}H$ NMR spectra of complex $1^{H}$ (bottom), $1^{H}$ in the presence of 4 equiv. TBAB (Middle) and $1^{H}$ in the presence of 4 equiv. TBAB and 12 eq. SO (Top) in DMSO-$d_6$ (δH 2.50 ppm). ..... 52

Figure S78: $^{1}H$ NMR spectrum of Zn-$1^{H}$/TBAB (1:4) added styrene oxide (SO) and $CS_2$ at $22^{0}C$, NMR taken after 1 h. interval in DMSO-$d_6$. ..... 53

Figure S79: FT-IR spectrum of cyclic cyclohexane carbonate CHO(*cis*) synthesized using Zn-$1^{H}$ as catalyst(Table 5, Reaction 2). ..... 53

Table S1: Crystallographic data parameters. ..... 53

Table S2: Comparison of cyclic CHC formation by the reaction of CHO and $CO_2$ using Zn complex as a catalyst ..... 54

Table S3: Important references related to the selective cyclic carbonate formation by the reaction of $CO_2$ cycloaddition to epoxide. ..... 55

Table S4: Important references related to the selective cyclic thio-carbonate formation by the reaction of $CS_2$ cycloaddition to epoxide. ..... 56

Note on the Crystal structure analysis for $H_2L^{NO2}$: ..... 60

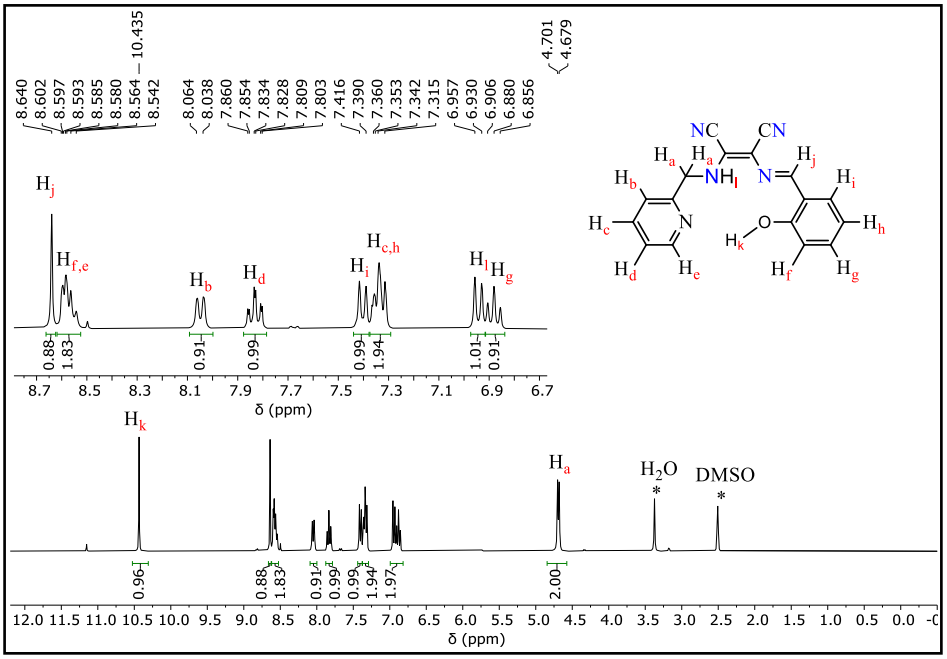


Figure S1: $^{1}$H NMR Spectrum of $H_2L^H$ in DMSO- $d_6$.

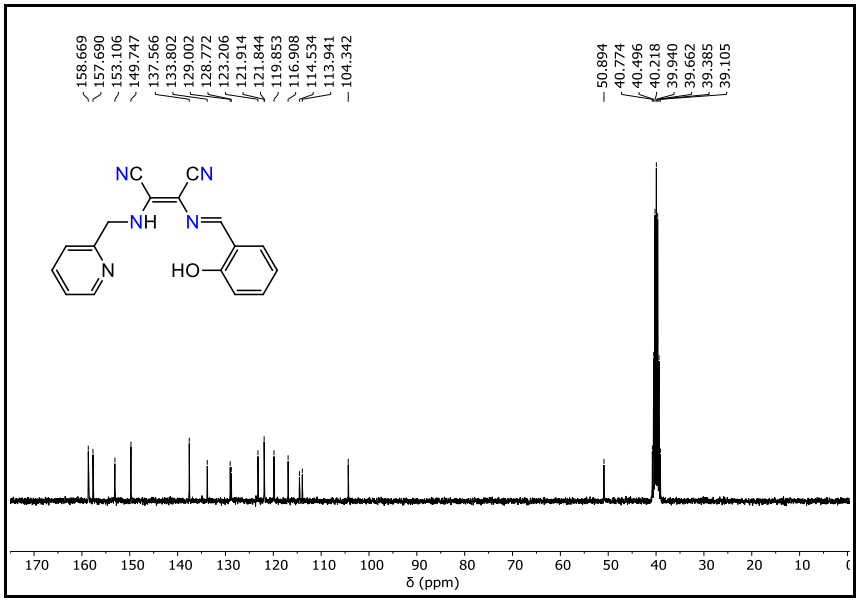

Figure S2: $^{13}C$ NMR Spectrum of $H_2L^H$ in DMSO- $d_6$.

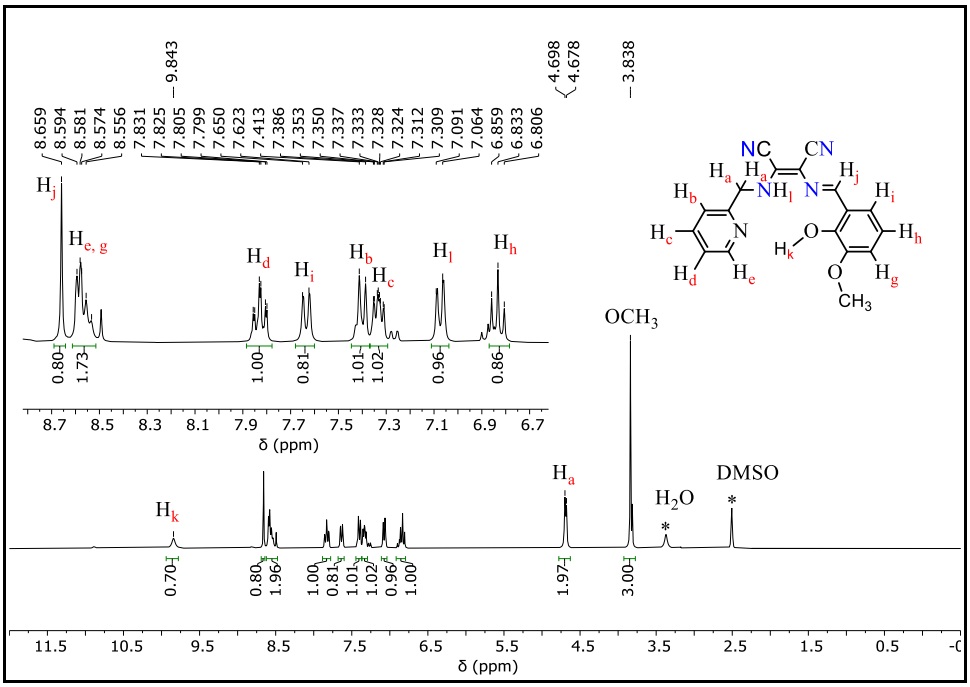


Figure S3: $^{1}H$ NMR Spectrum of $H_2L^{OMe}$ in DMSO- $d_6$.

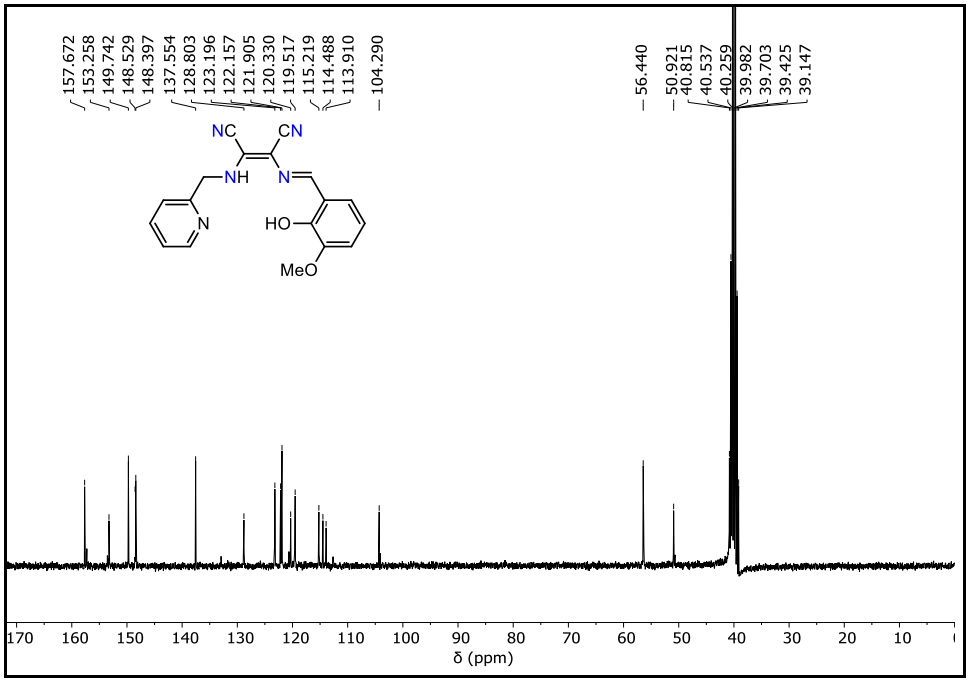

Figure S4: $^{13}C$ NMR Spectrum of $H_2L^{OMe}$ in DMSO- $d_6$.

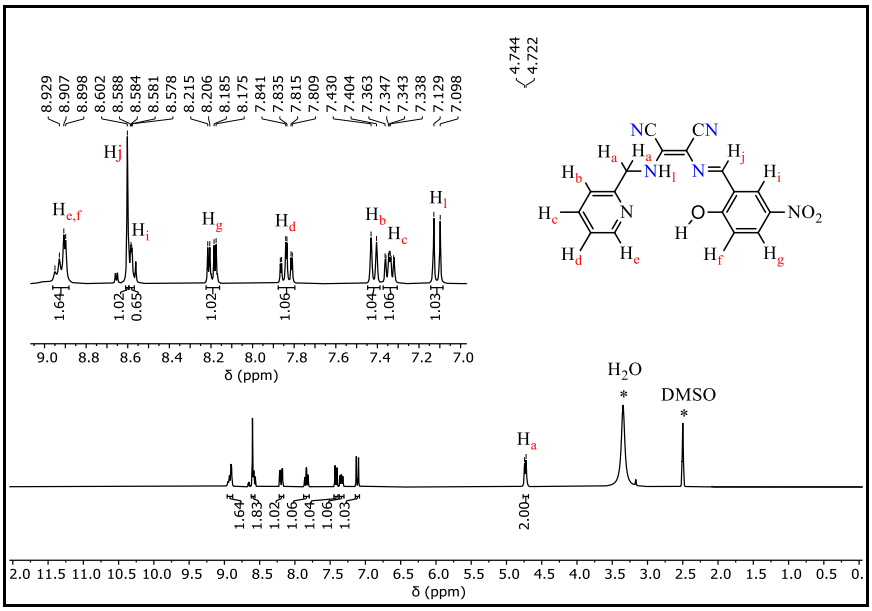


Figure S5: $^{1}H$ NMR Spectrum of $H_2L^{NO2}$ in DMSO- $d_6$.

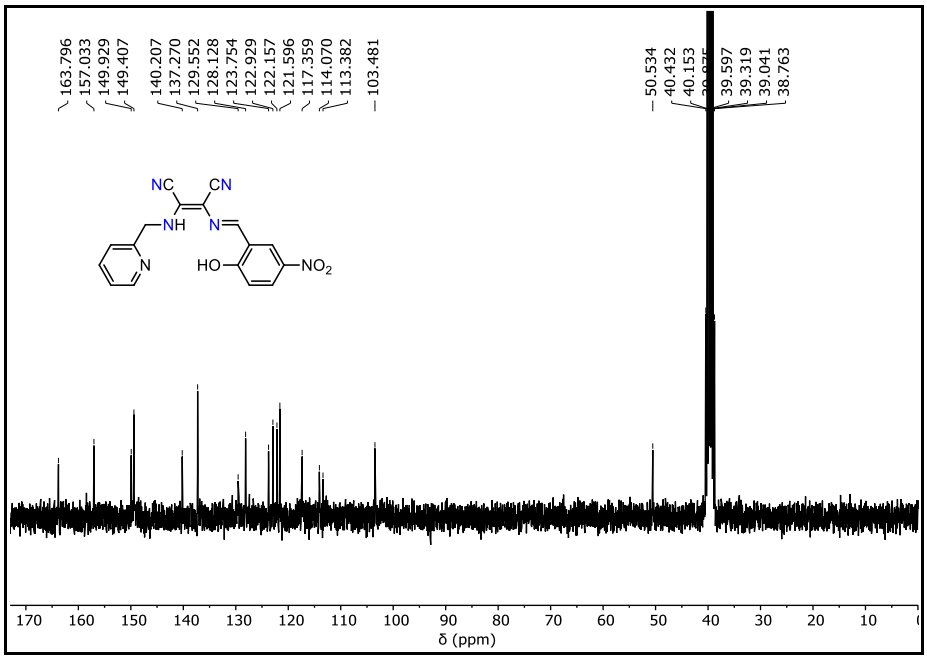

Figure S6: $^{13}C$ NMR Spectrum of $H_2L^{NO2}$ in DMSO- $d_6$.

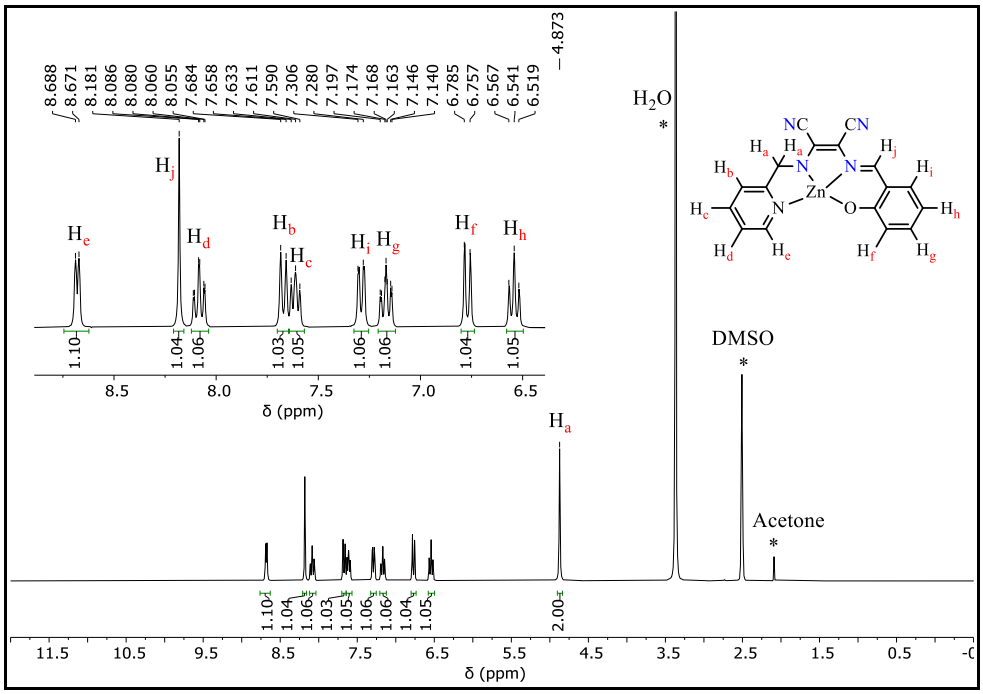


Figure S7: $^{1}H$ NMR Spectrum of [Zn($L^{H}$)] in DMSO- $d_6$.

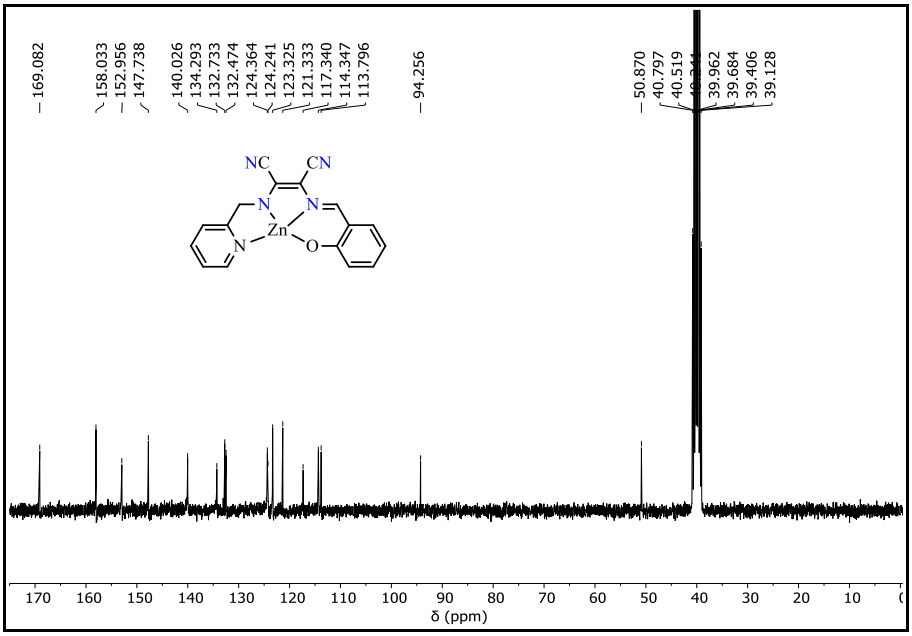

Figure S8: $^{13}C$ NMR Spectrum of [Zn($L^{H}$)] in DMSO- $d_6$.

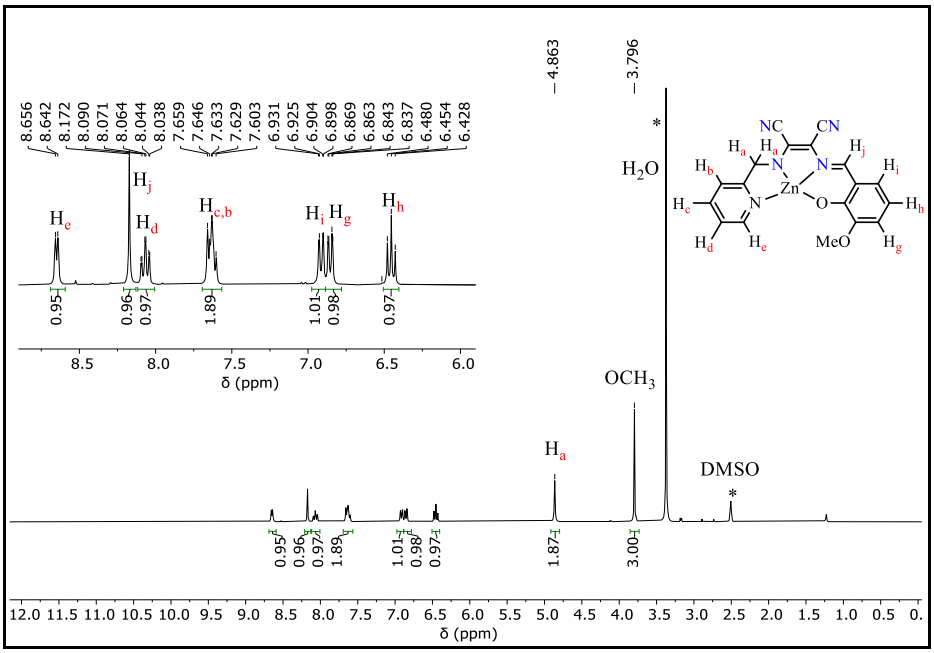


Figure S9: $^{1}H$ NMR Spectrum of [Zn($L^{OMe}$)] in DMSO- $d_6$.

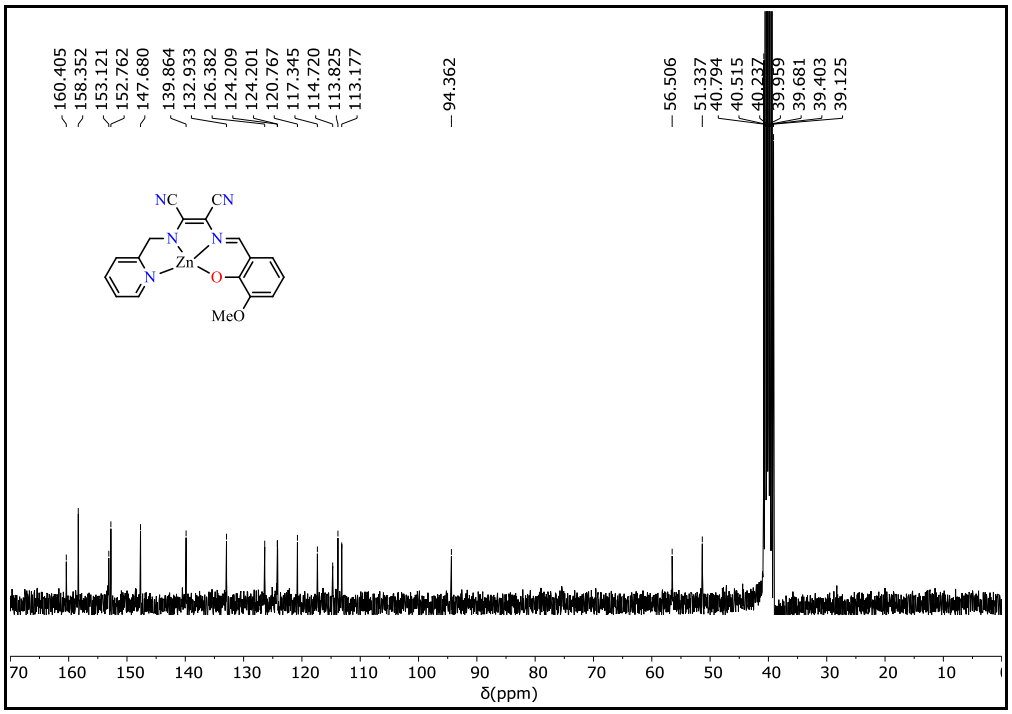

Figure S10: $^{13}$C NMR Spectrum of [Zn($L^{OMe}$)] in DMSO- $d_6$.

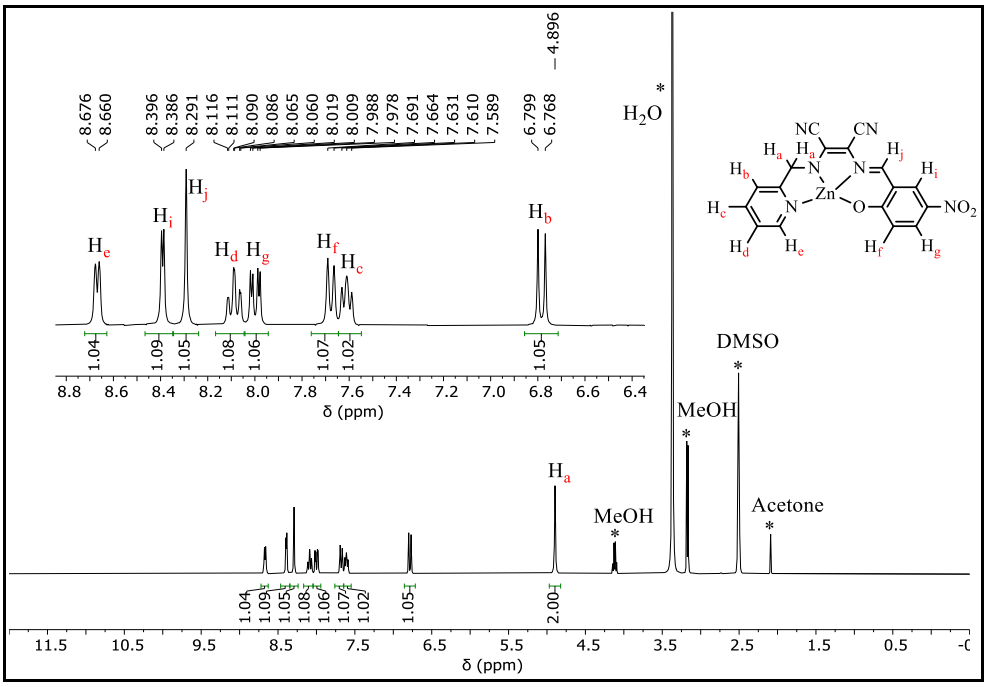


Figure S11: $^{1}$H NMR Spectrum of [Zn($L^{NO2}$)] in DMSO- $d_6$.

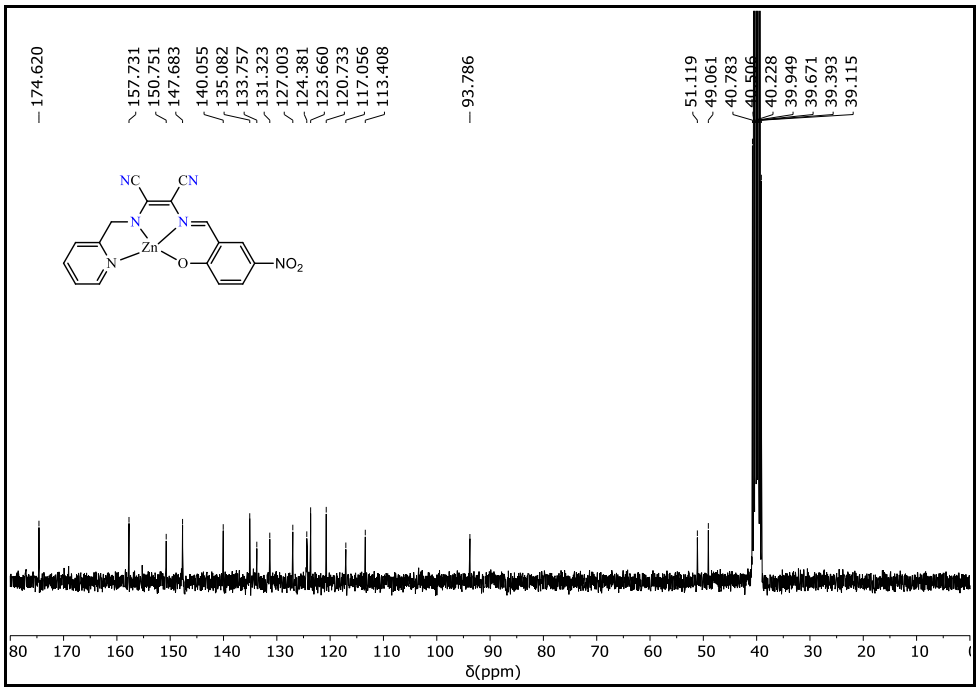

Figure S12: $^{13}$C NMR Spectrum of [Zn($L^{NO2}$)] in DMSO- $d_6$.

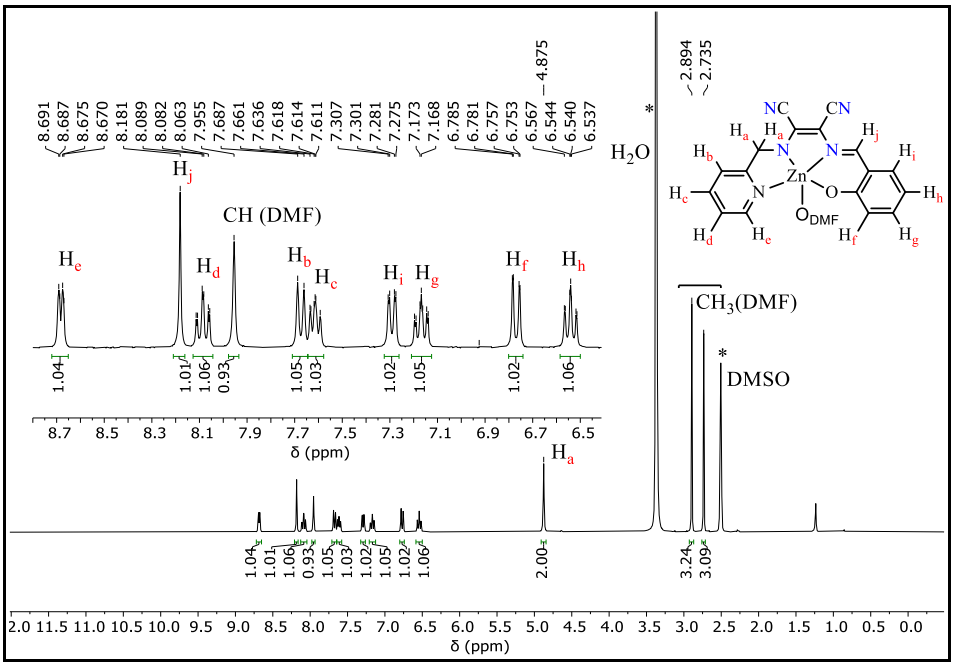


Figure S13: $^{1}$H NMR Spectrum of [Zn($L^{H}$)(DMF)] in DMSO- $d_6$.

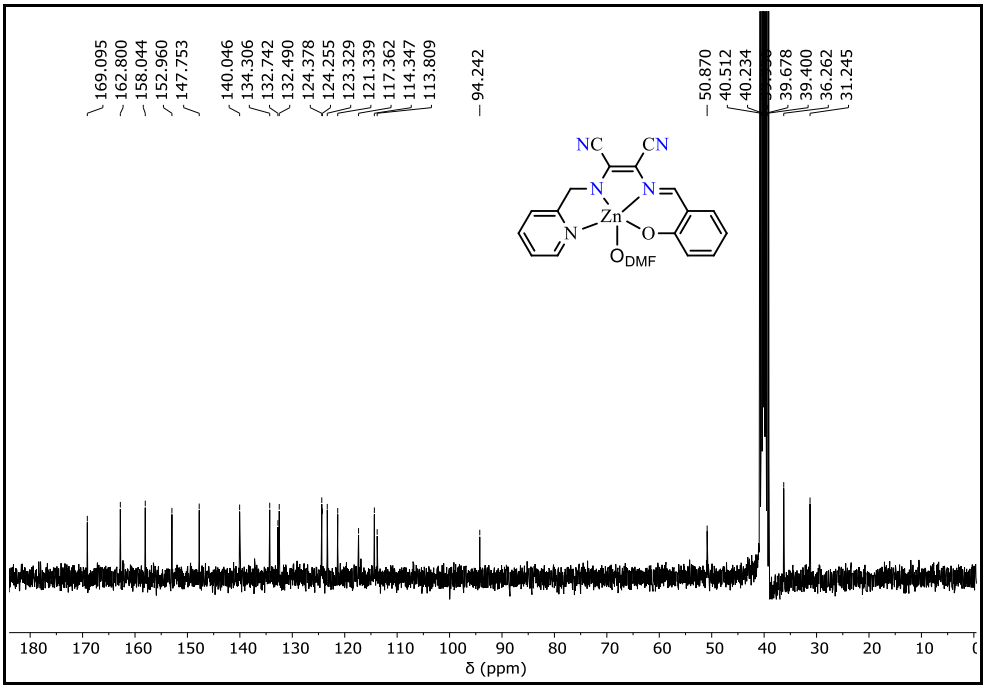

Figure S14: $^{13}C$ NMR Spectrum of [Zn($L^{H}$)(DMF)] in DMSO- $d_6$.

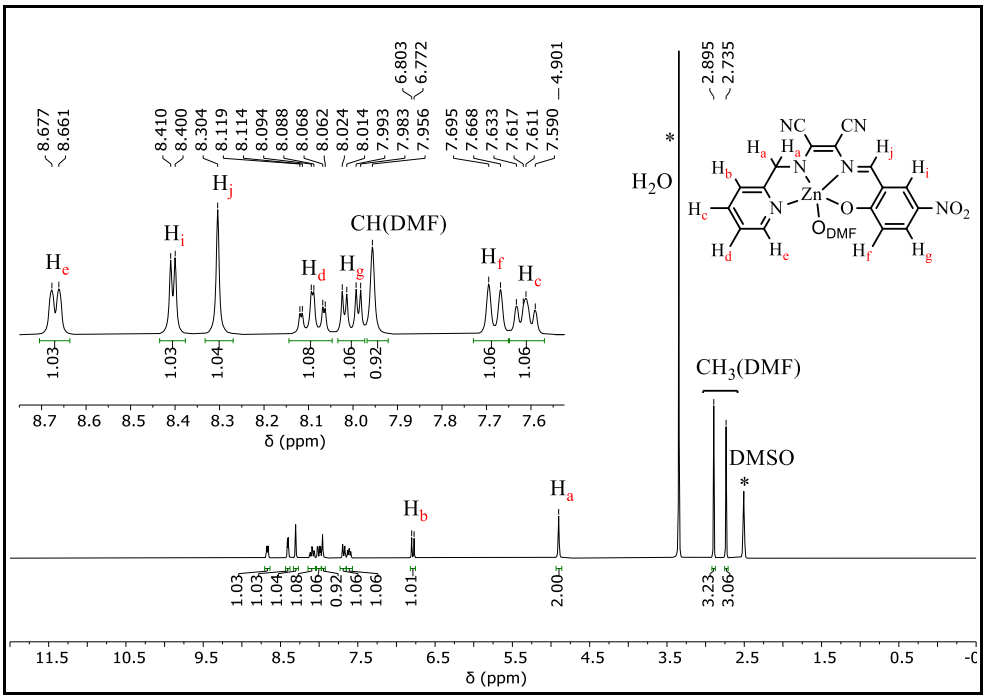


Figure S15: $^{1}H$ NMR Spectrum of [Zn($L^{NO2}$)(DMF)] in DMSO- $d_6$.

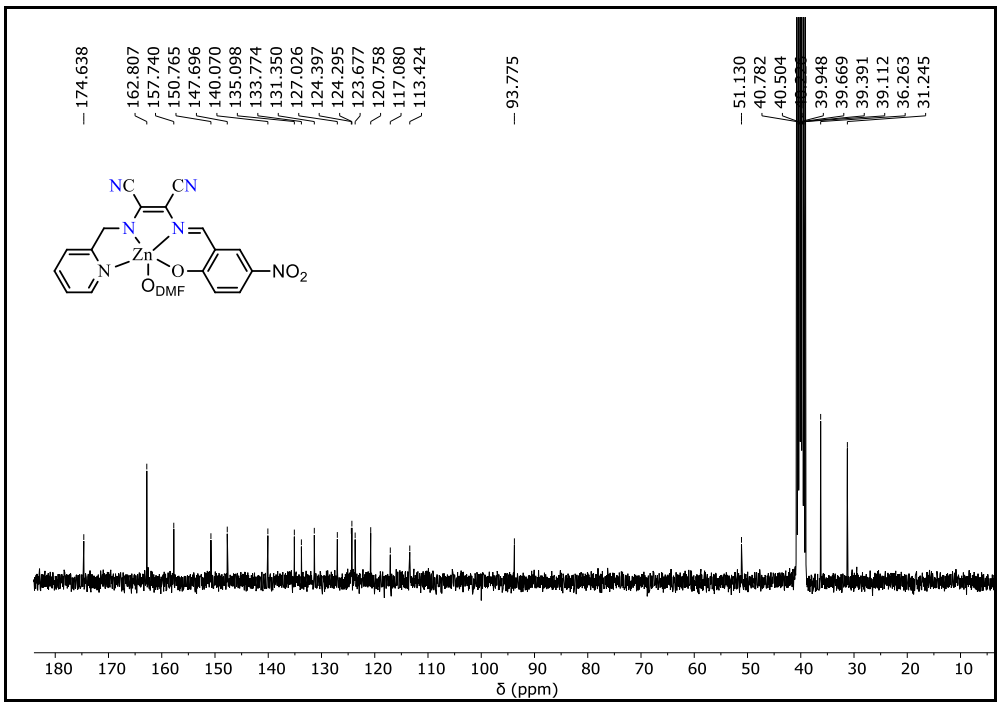

Figure S16: $^{13}$C NMR Spectrum of [Zn($L^{NO2}$)(DMF)] in DMSO- $d_6$.

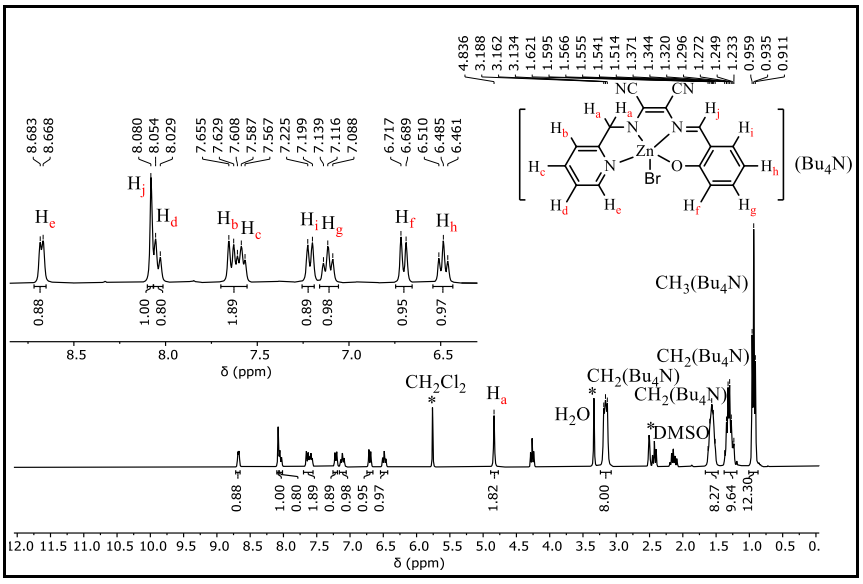


Figure S17: $^{1}$H NMR Spectrum of [Zn($L^{H}$)Br](Bu$_4$N) in DMSO-$d_6$.

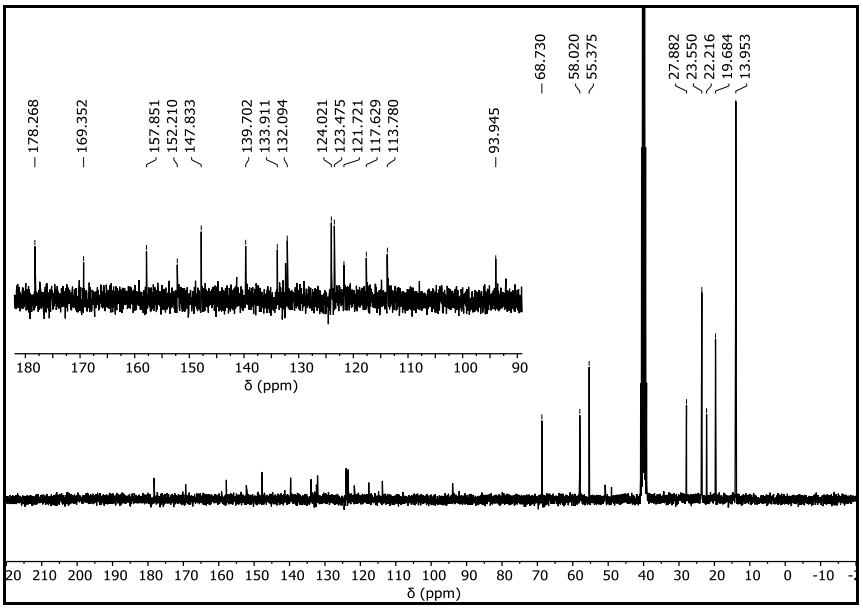


Figure S18: $^{13}$C NMR Spectrum of [Zn($L^{H}$)Br](Bu$_4$N) in DMSO-$d_6$.

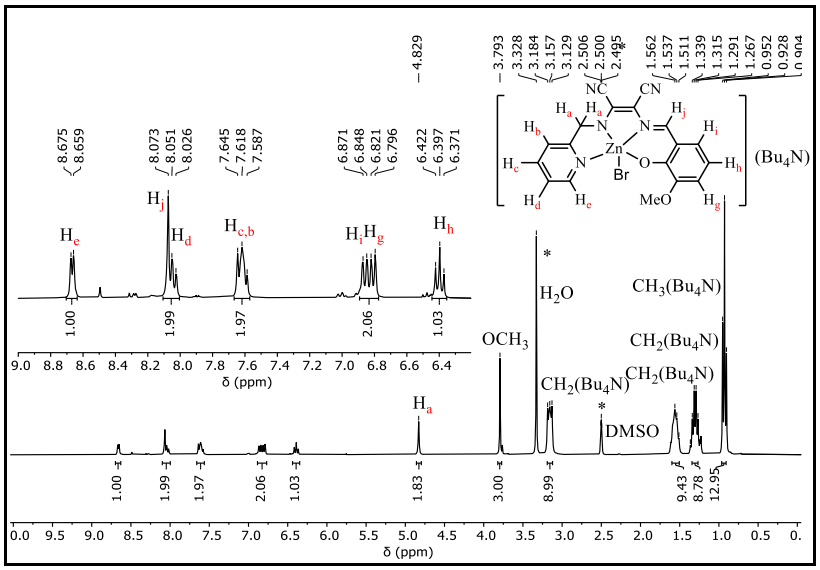

Figure S19: $^{1}$H NMR Spectrum of [Zn(L$^{OMe}$)Br](Bu$_4$N) in DMSO-$d_6$.

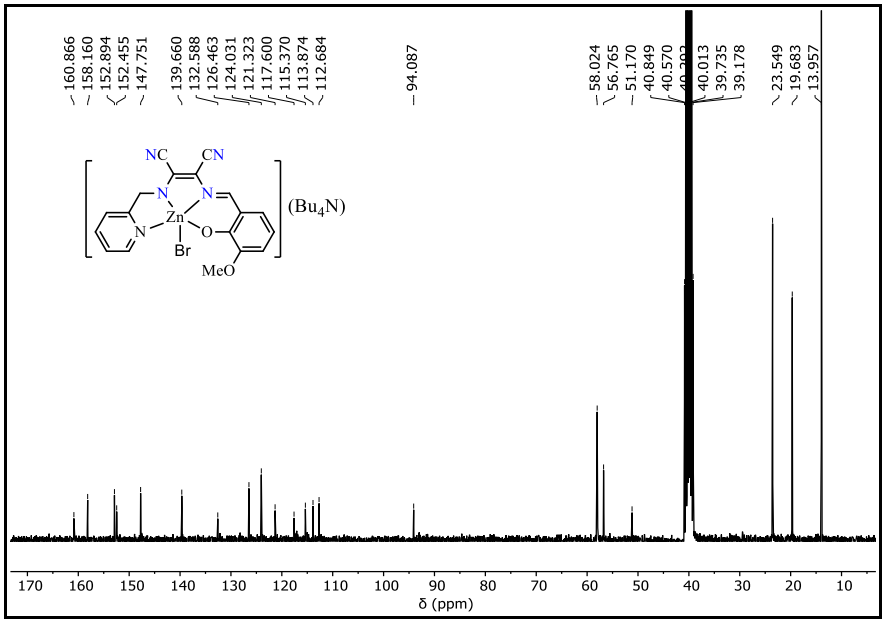

Figure S20: $^{13}$C NMR Spectrum of [Zn(L$^{OMe}$)Br](Bu$_4$N) in DMSO-$d_6$.

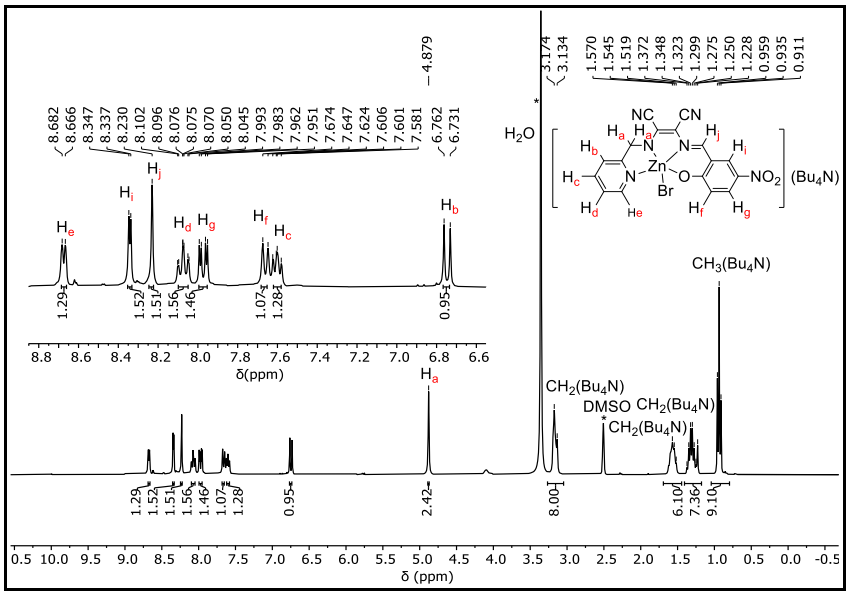

Figure S21: $^{1}$H NMR Spectrum of [Zn($L^{NO2}$)Br](Bu$_4$N) in DMSO-$d_6$.

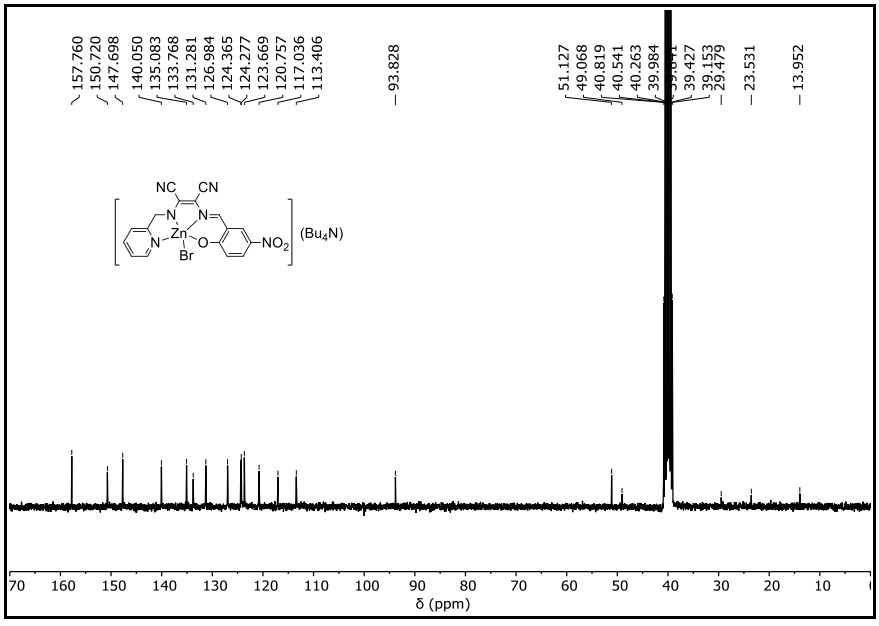

Figure S22: $^{13}$C NMR Spectrum of [Zn($L^{NO2}$)Br](Bu$_4$N) in DMSO-$d_6$.

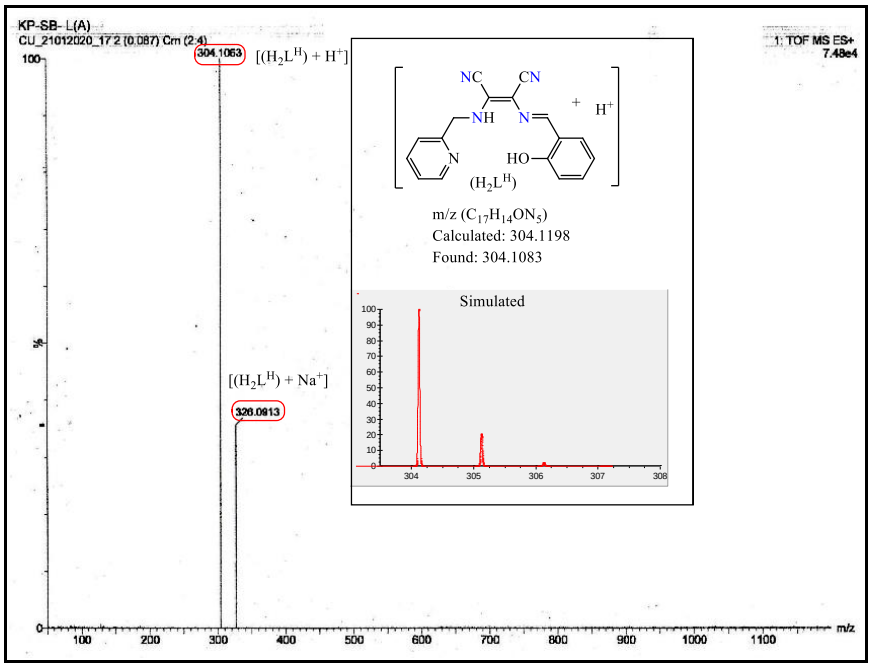


Figure S23: ESI-MS spectrum of $H_2L^H$.

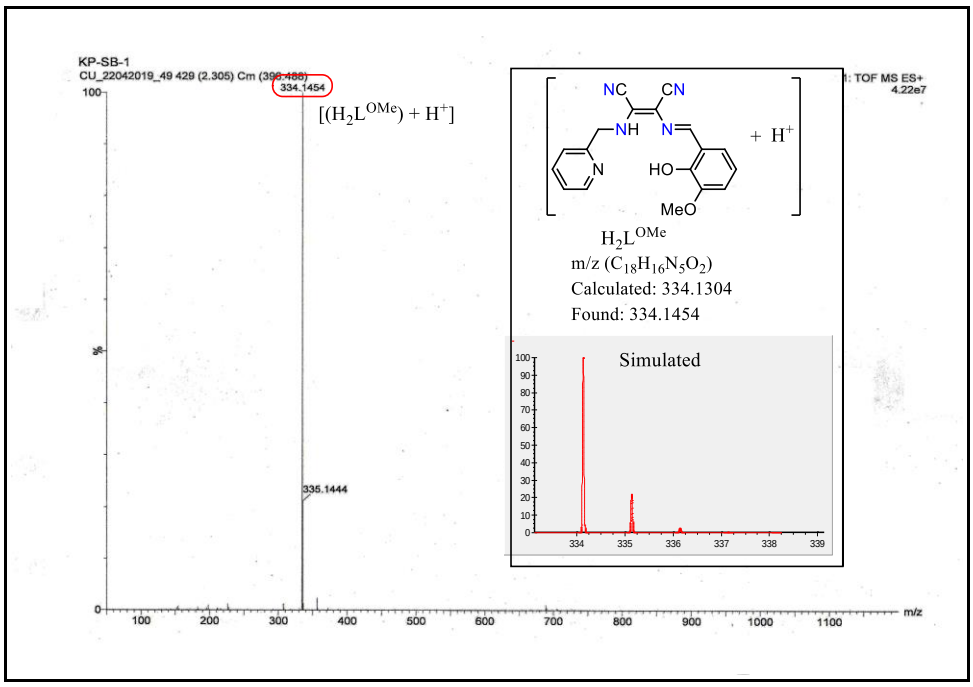

Figure S24: ESI-MS spectrum of $H_2L^{OMe}$.

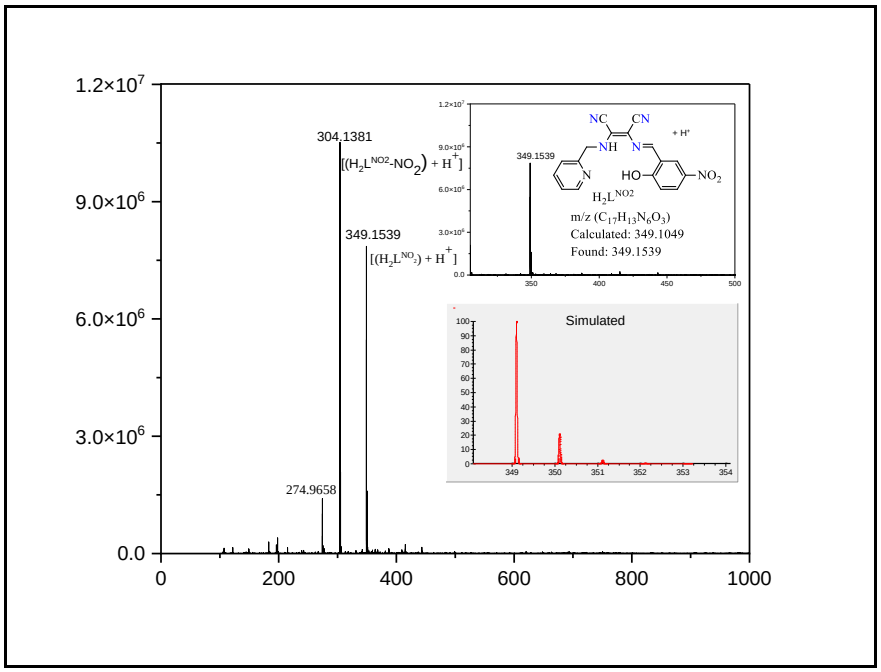


Figure S25: ESI-MS spectrum of $H_2L^{NO2}$.

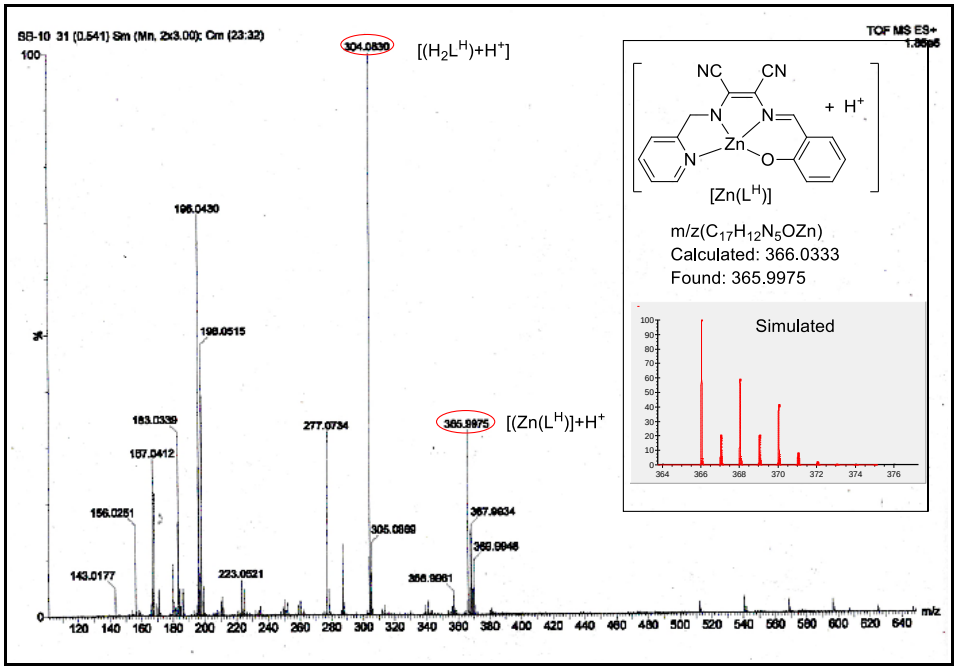

Figure S26: ESI-MS Spectrum of [Zn($L^{H}$)].

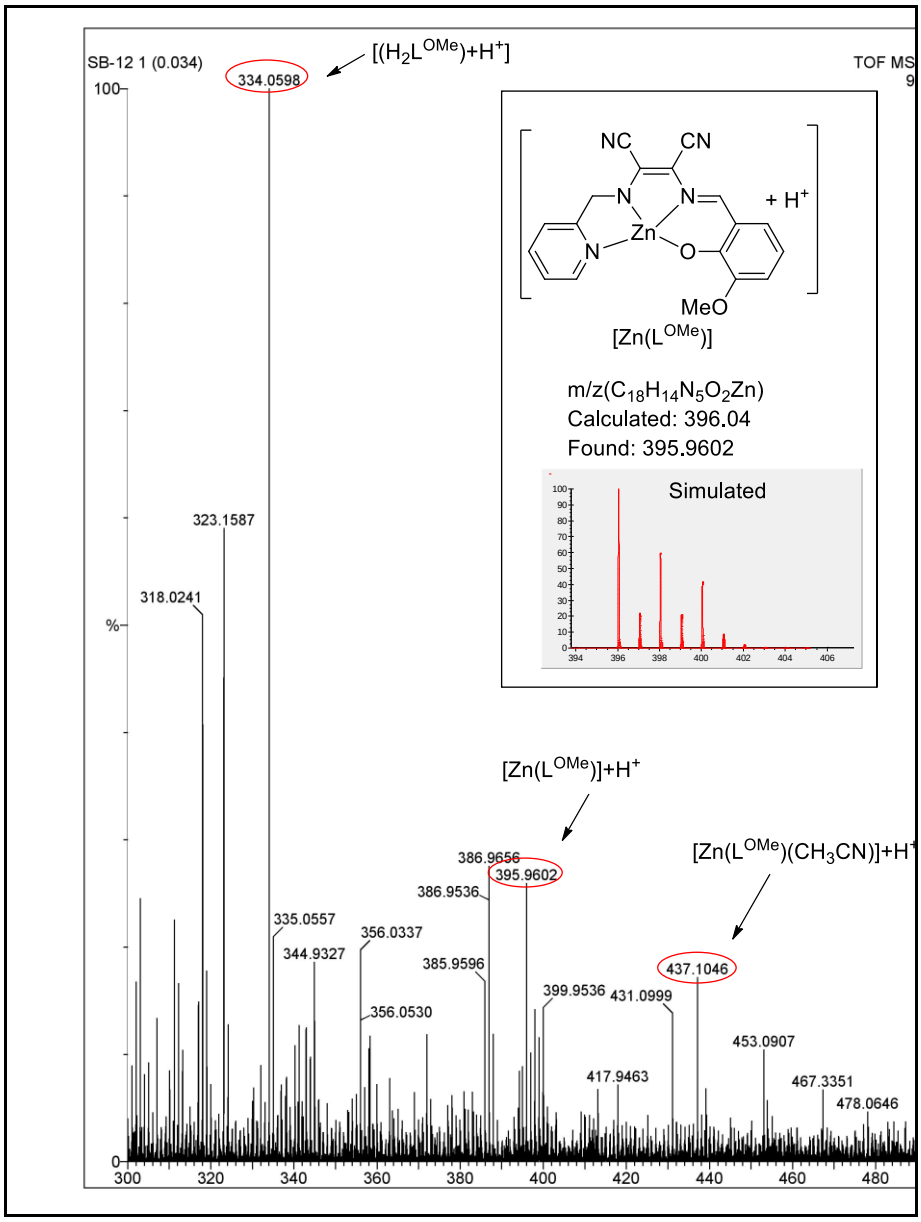


Figure S27: ESI-MS Spectrum of [Zn($L^{OMe}$)].

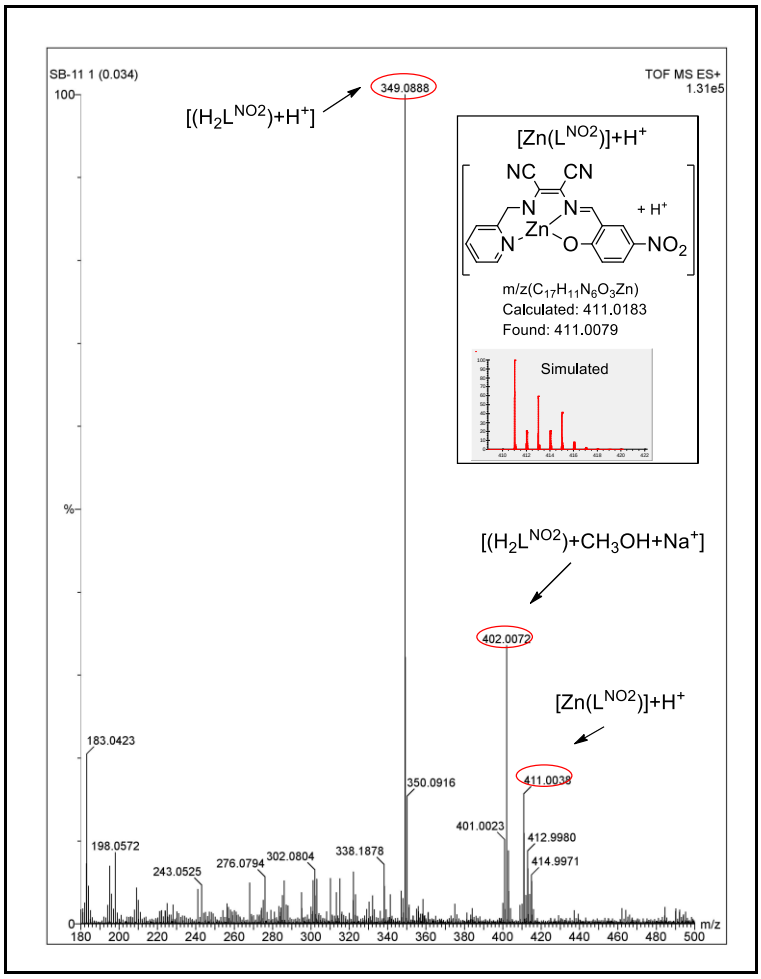


Figure S28: ESI-MS Spectrum of [Zn($L^{NO2}$)].

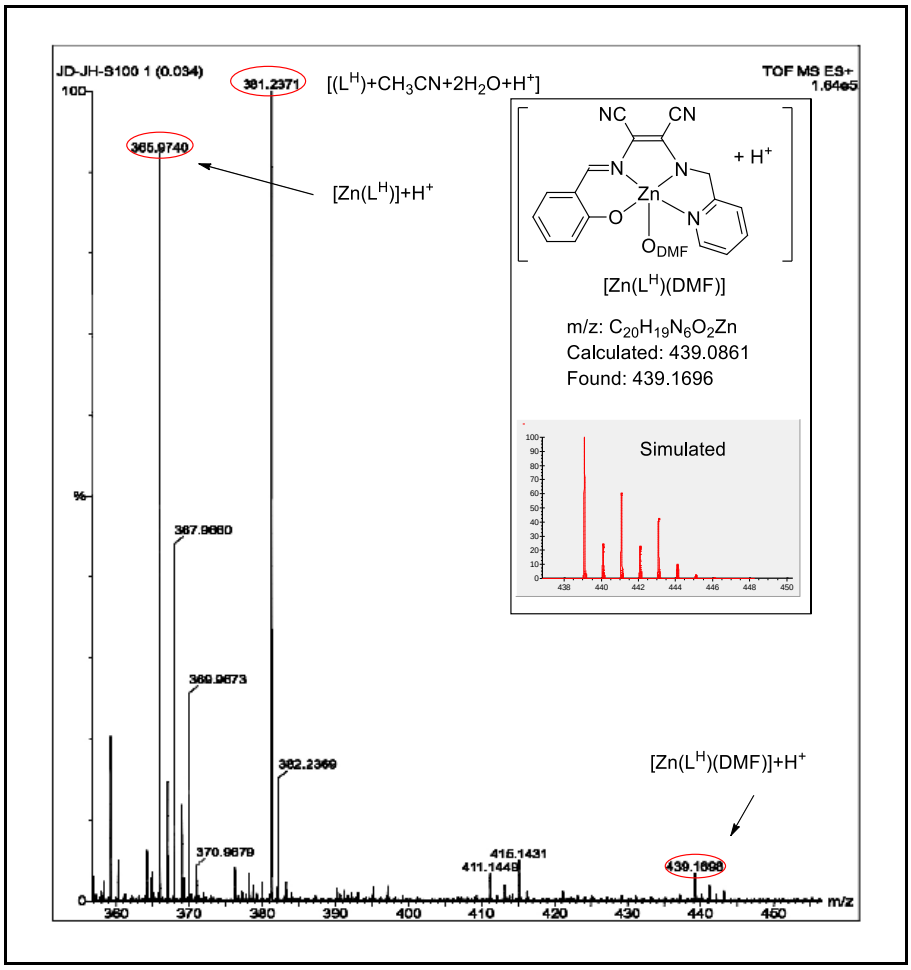


Figure S29: ESI-MS Spectrum of [Zn($L^H$)(DMF)].

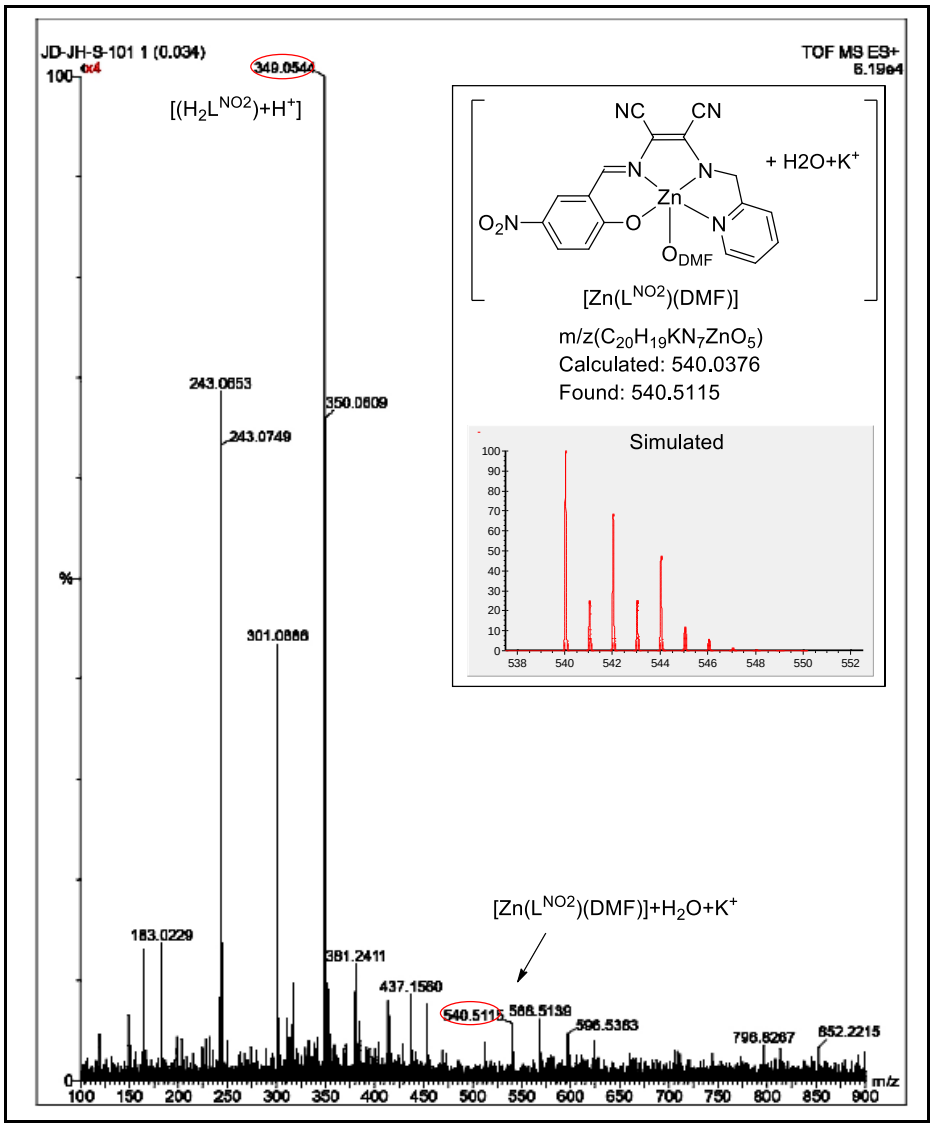


Figure S30: ESI-MS Spectrum of [Zn($L^{NO2}$)(DMF)].

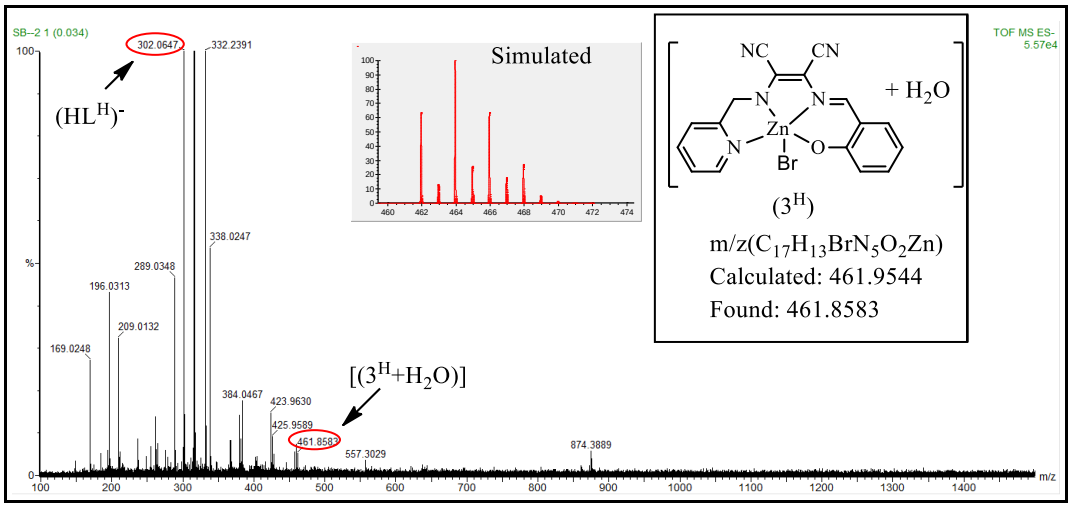


Figure S31: ESI-MS Spectrum of [Zn($L^{H}$)Br]($Bu_4N$).

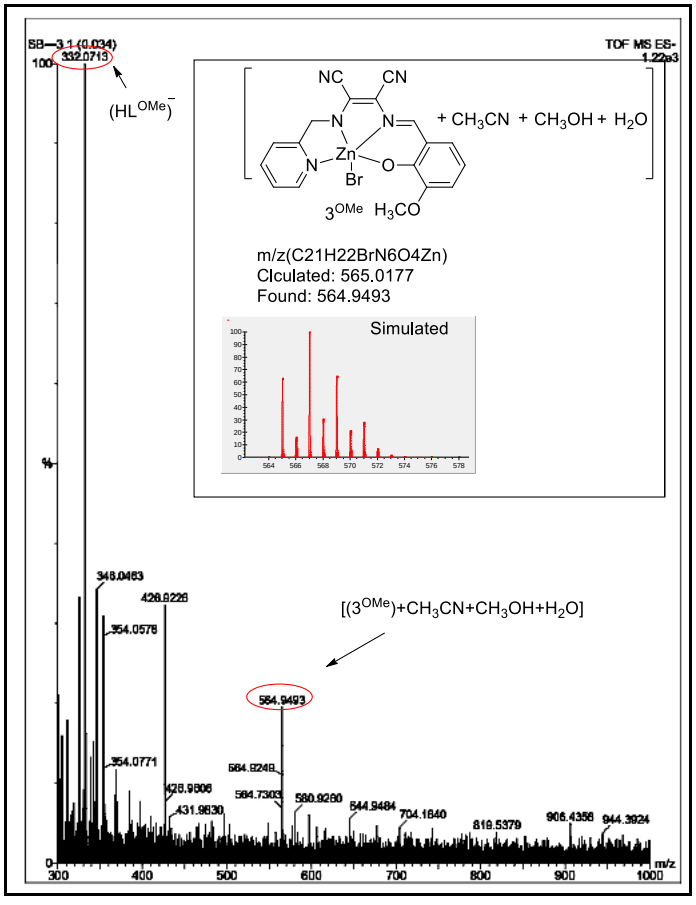


Figure S32: ESI-MS Spectrum of [Zn($L^{OMe}$)Br]($Bu_4N$).

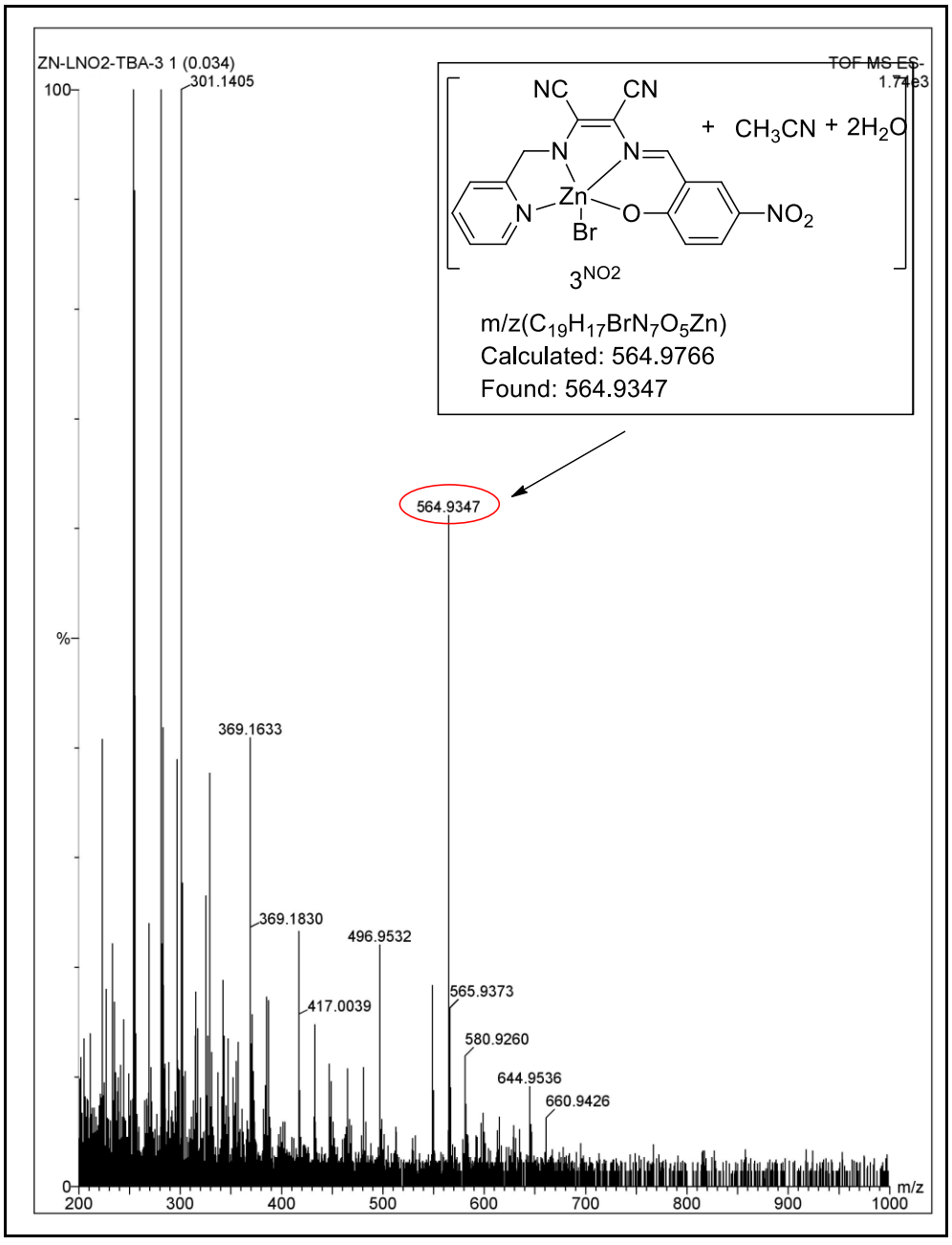


Figure S33: ESI-MS Spectrum of [Zn($L^{NO2}$)Br]($Bu_4N$).

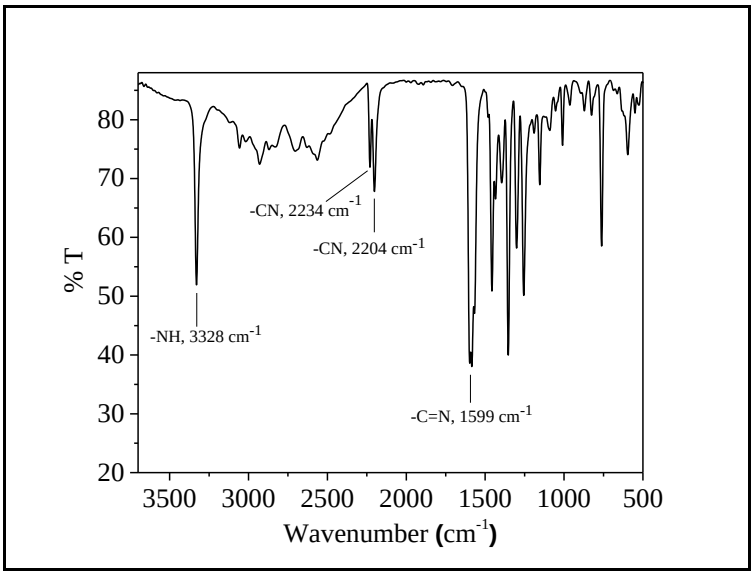


Figure S34: FT-IR spectrum of $H_2L^H$.

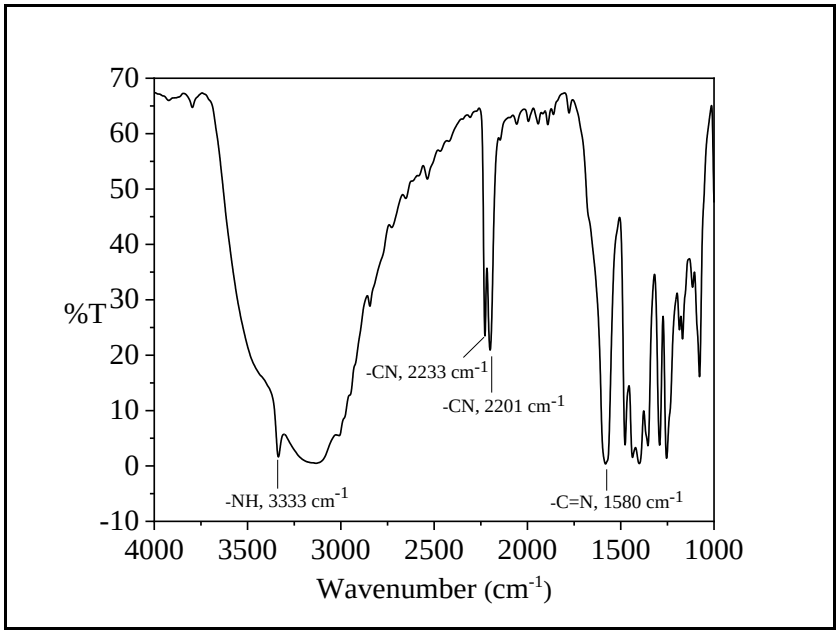


Figure S35: FT-IR spectrum of $H_2L^{OMe}$.

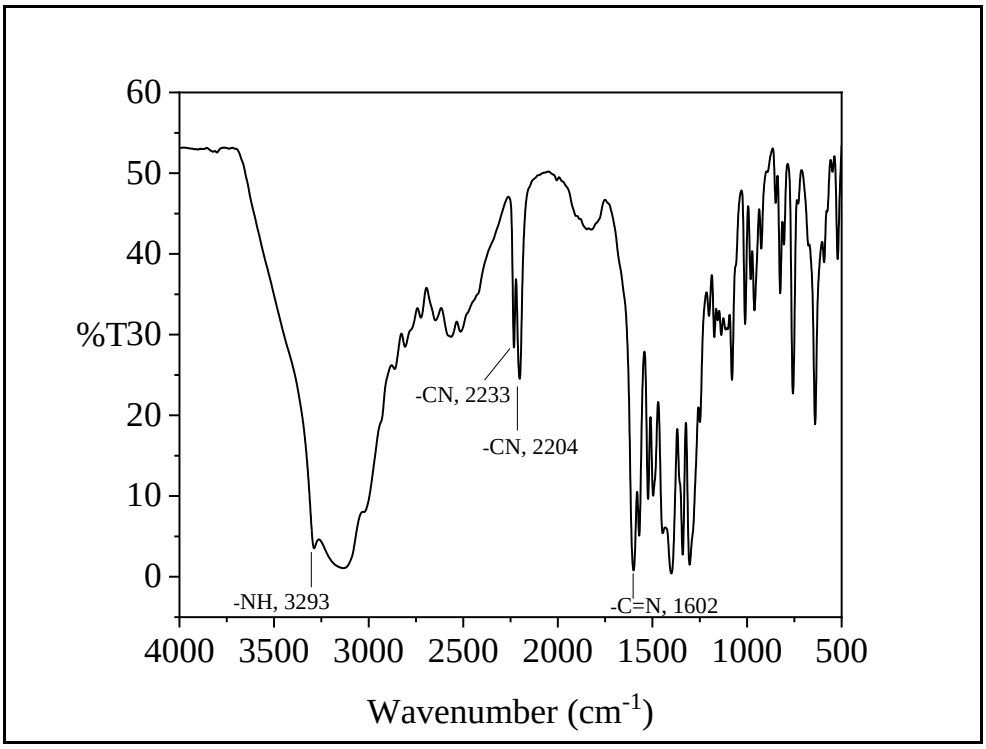


Figure S36: FT-IR spectrum of $H_2L^{NO2}$.

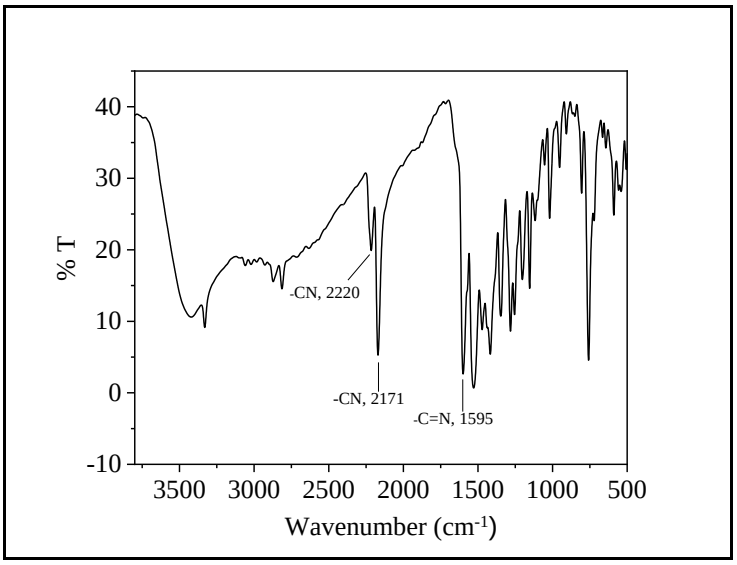


Figure S37: FT-IR Spectrum of [Zn($L^H$)].

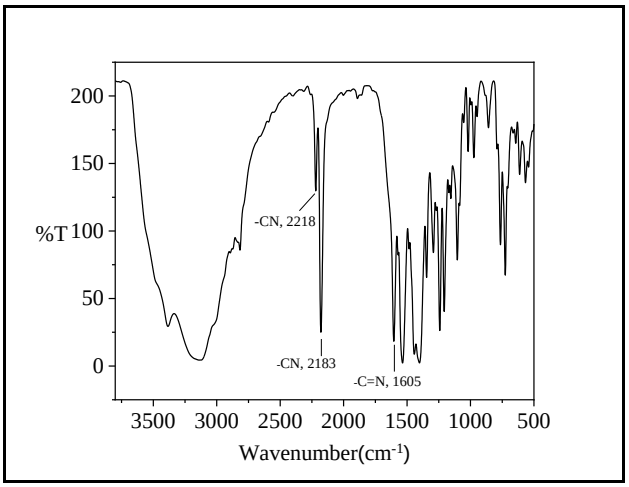


Figure S38: FT-IR Spectrum of [Zn($L^{OMe}$)].

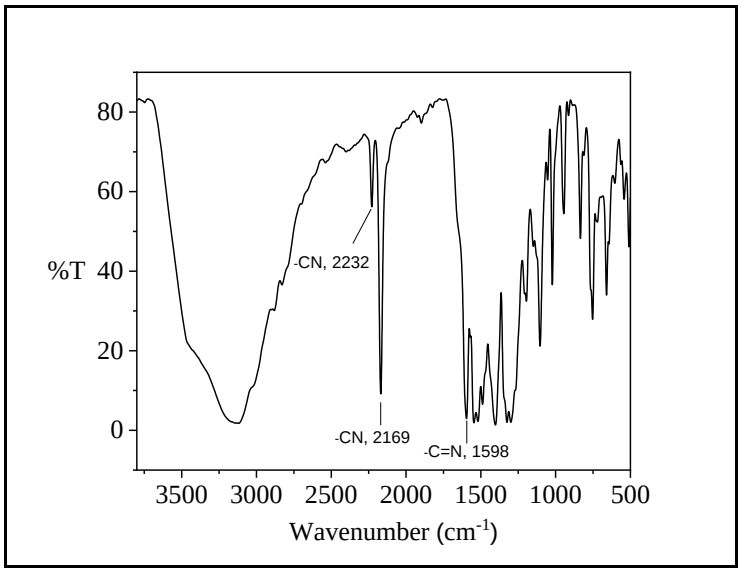


Figure S39: FT-IR Spectrum of [Zn($L^{NO2}$)].

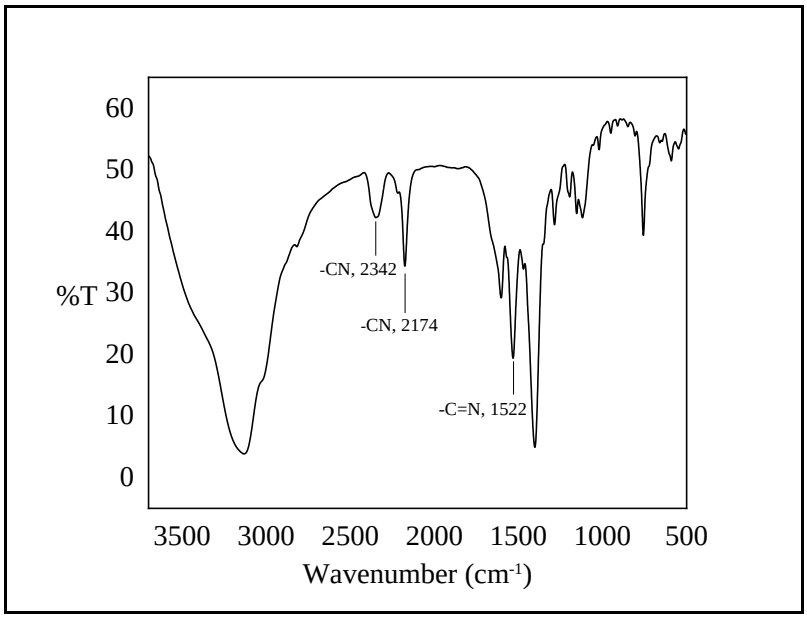


Figure S40: FT-IR Spectrum of [Zn($L^{H}$)(DMF)].

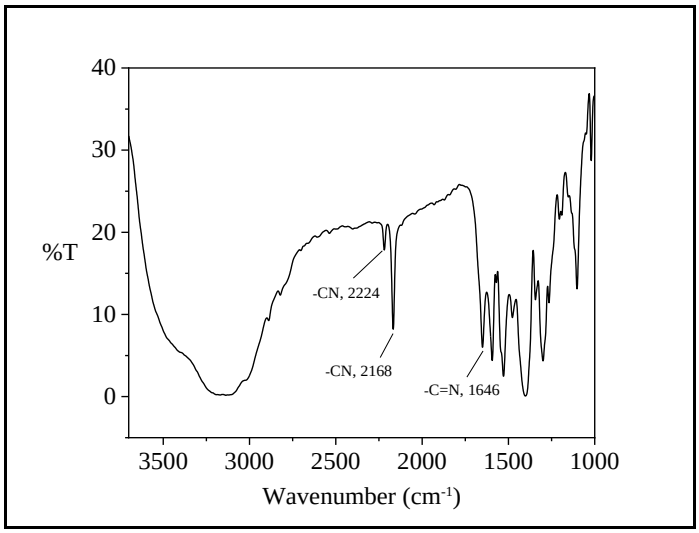


Figure S41: FT-IR Spectrum of [Zn($L^{NO2}$)(DMF)].

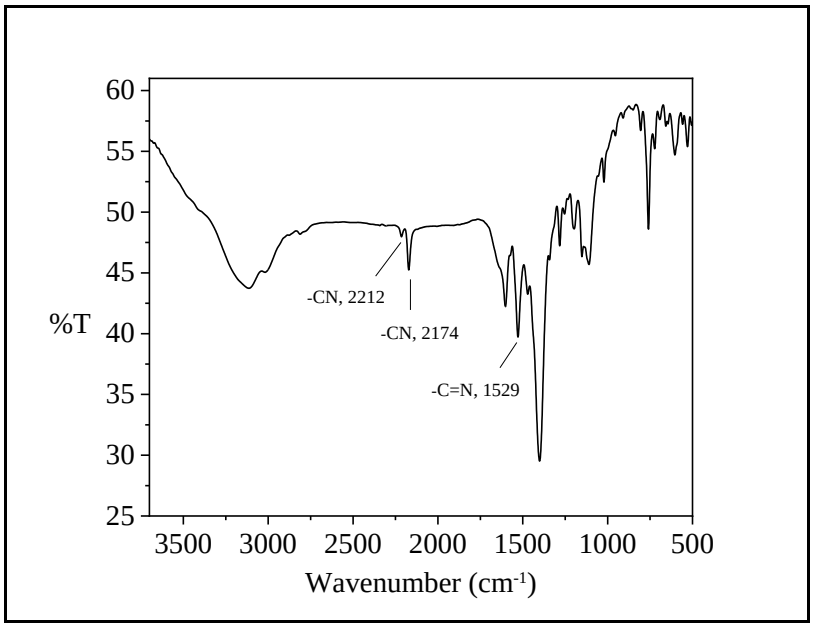


Figure S42: FT-IR Spectrum of [Zn($L^{H}$)Br]($Bu_4N$).

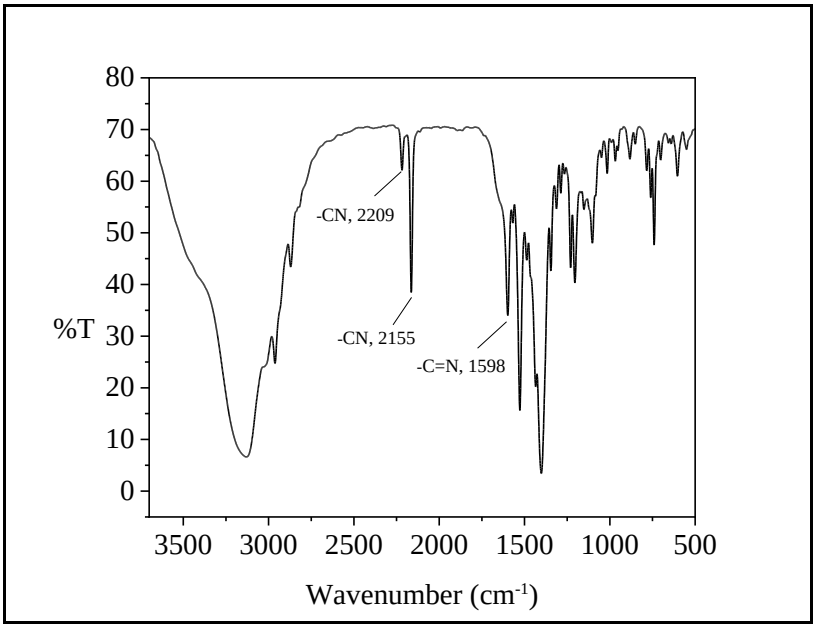


Figure S43: FT-IR Spectrum of [Zn($L^{OMe}$)Br]($Bu_4N$).

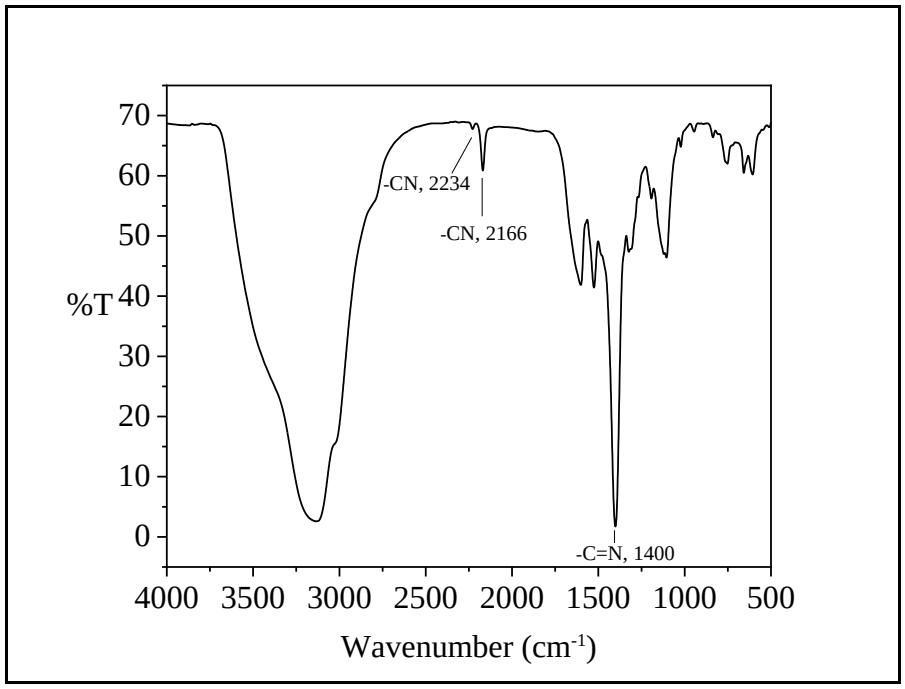


Figure S44: FT-IR Spectrum of $[Zn(L^{NO2})Br](Bu_4N)$.

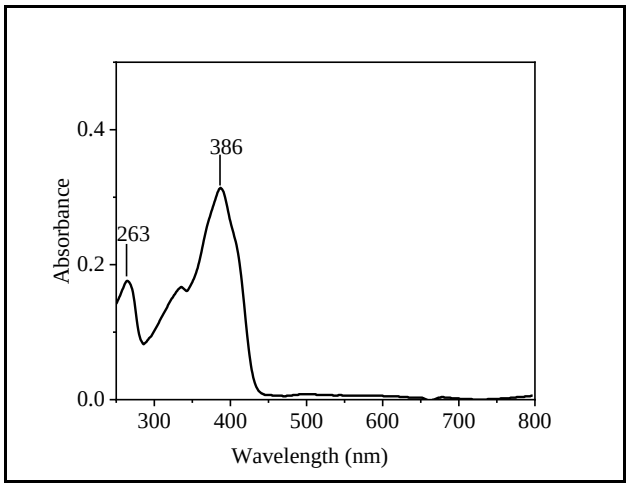


Figure S45: Electronic absorption spectra of $H_2L^H$ (1 x $10^{-5}$(M) in $CH_3CN$).

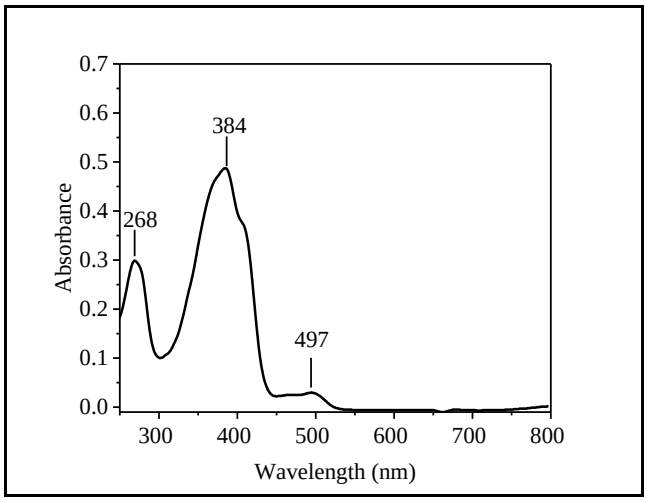


Figure S46: Electronic absorption spectra of $H_2L^{OMe}$ (5 x $10^{-5(}$M) in $CH_3CN$).

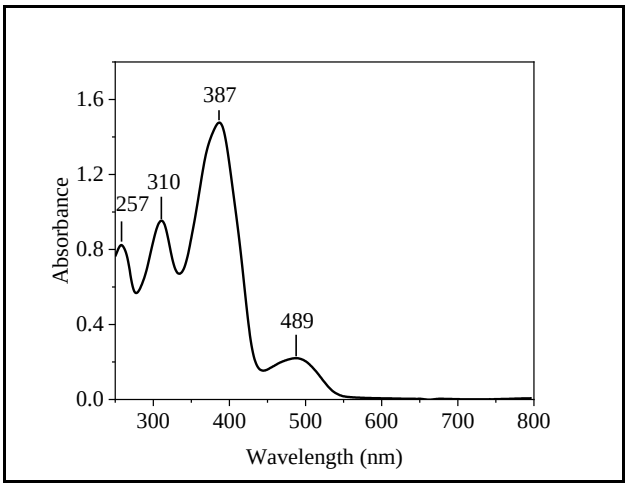


Figure S47: Electronic absorption spectra of $H_2L^{NO2}$ (5 x $10^{-5}$(M) in $CH_3CN$).

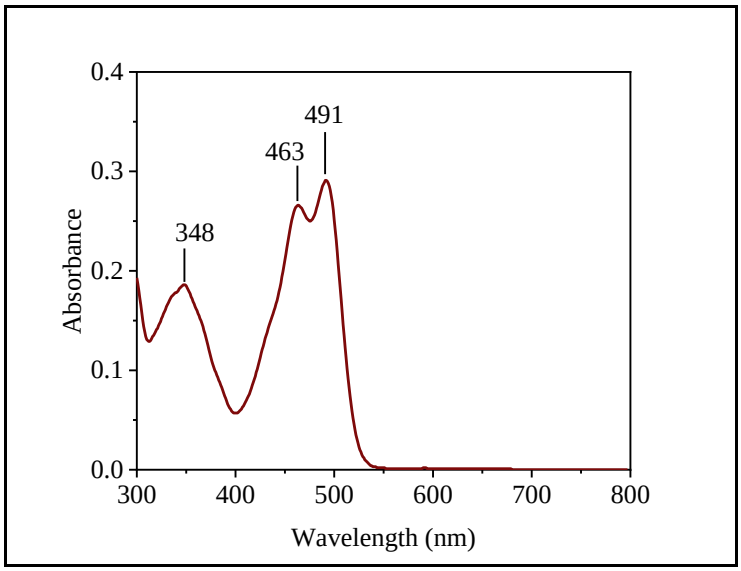


Figure S48: Electronic absorption spectra of [Zn($L^{H}$)] (1 x $10^{-5}$(M) in DMF).

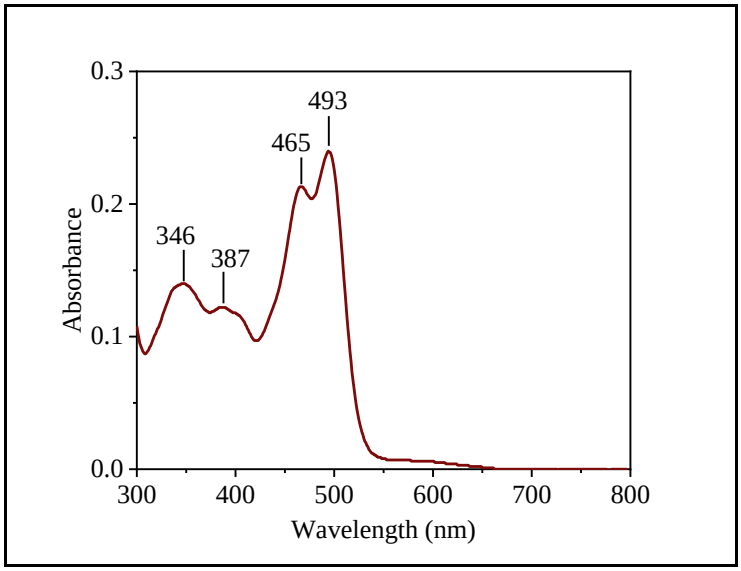


Figure S49: Electronic absorption spectra of [Zn($L^{OMe}$)] (1 x $10^{-5}$(M) in DMF).

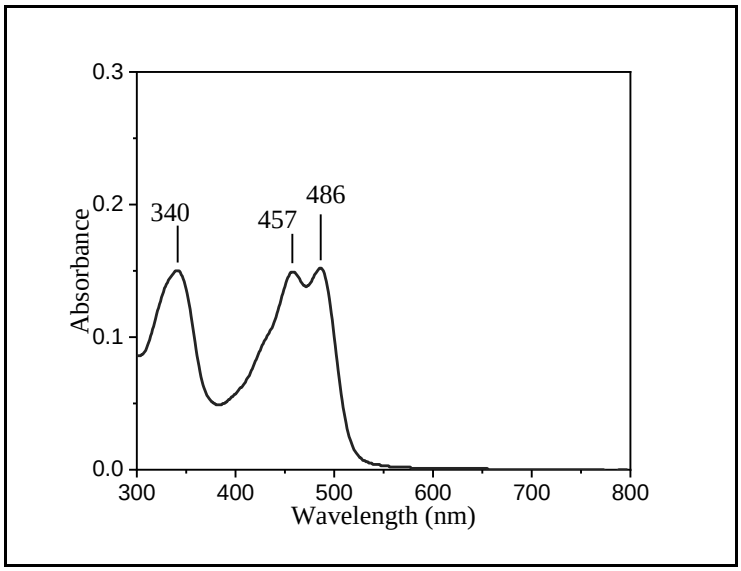


Figure S50: Electronic absorption spectra of [Zn($L^{NO2}$)] (1 x $10^{-5}$(M) in $CH_3CN$).

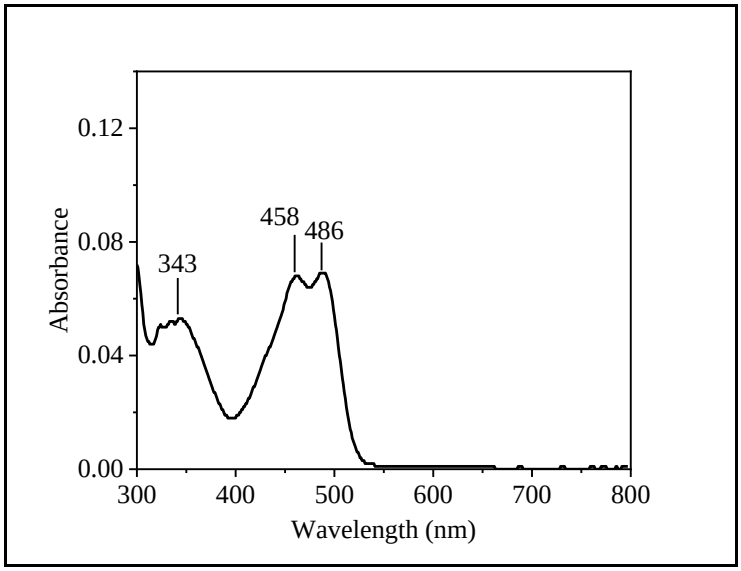


Figure S51: Electronic absorption spectra of [Zn($L^{H}$)(DMF)] (1 x $10^{-5}$(M) in $CH_3CN$).

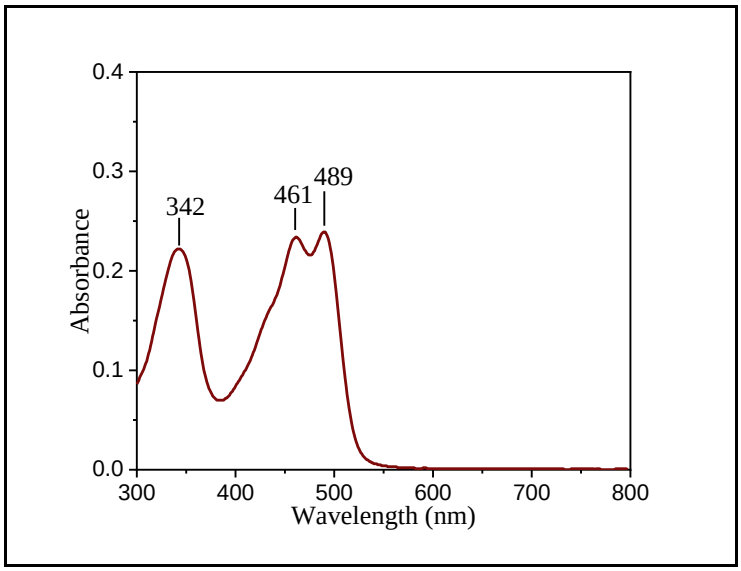


Figure S52: Electronic absorption spectra of [Zn($L^{NO2}$)(DMF)] (1 x $10^{-5}$(M) in DMF).

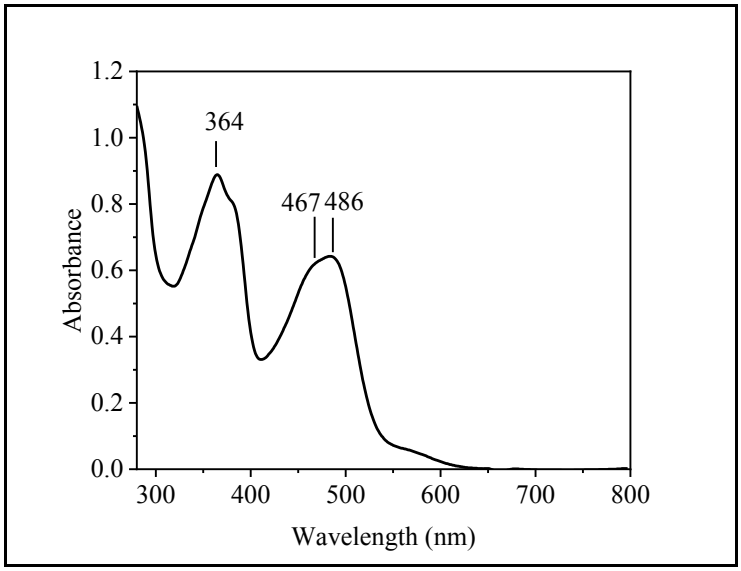


Figure S53: Electronic absorption spectra of [Zn($L^{H}$)Br]($Bu_4N$) (5 x $10^{-5(}$M) in $CH_3CN$).

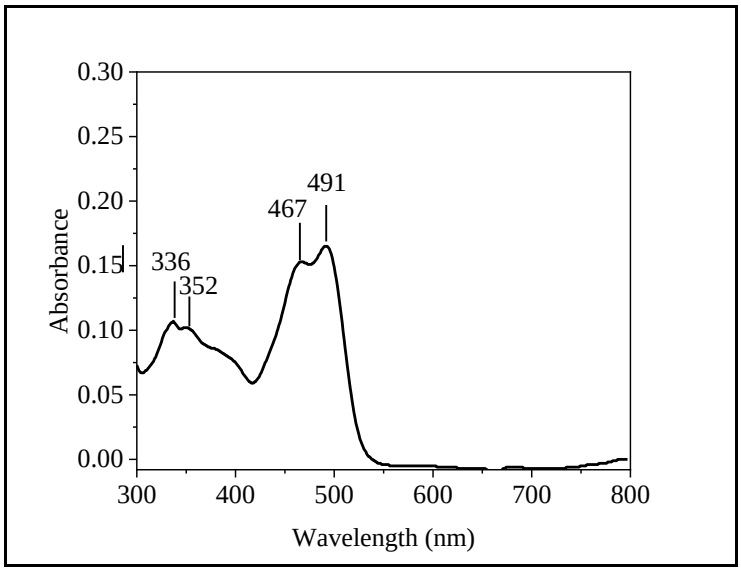


Figure S54: Electronic absorption spectra of [Zn($L^{OMe}$)Br]($Bu_4N$) (1 x $10^{-5}$(M**) in $CH_3CN$).**

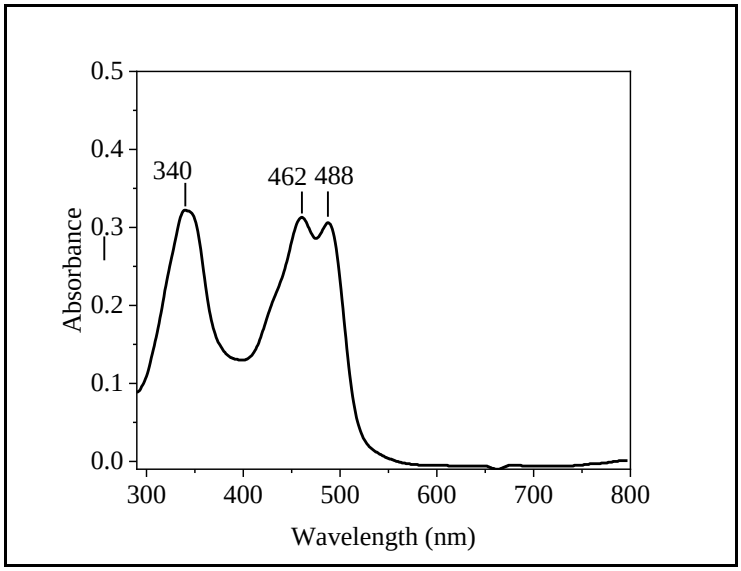


Figure S55: Electronic absorption spectra of [Zn($L^{NO2}$)Br]($Bu_4N$) (1 x $10^{-5}$(M) in $CH_3CN$).

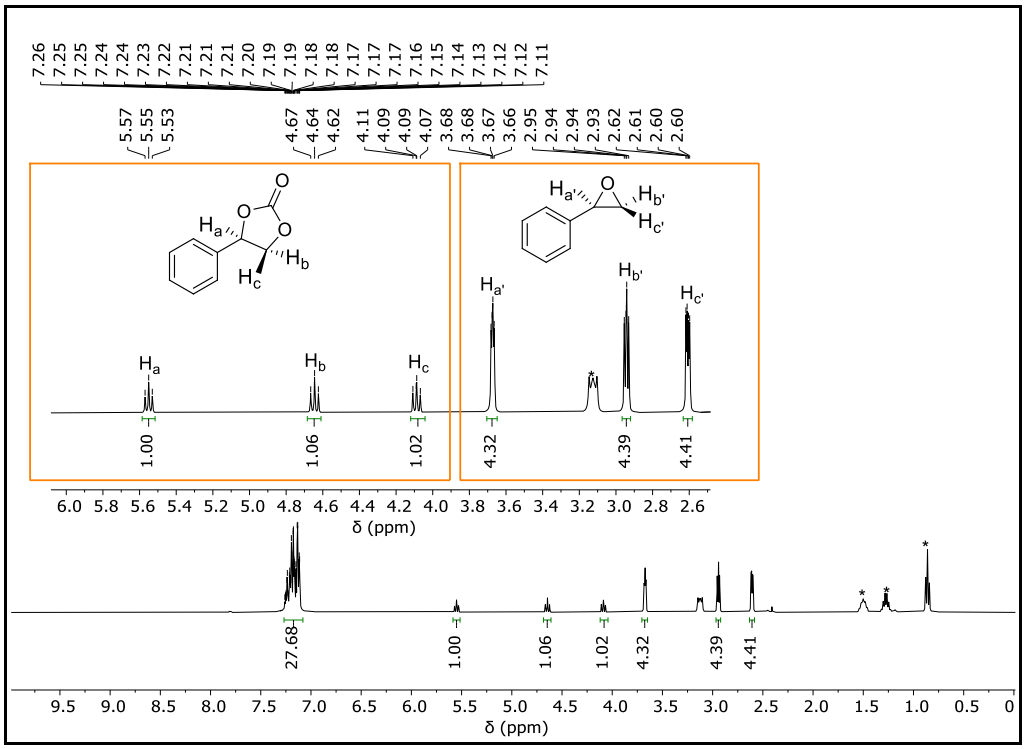


**Figure S56:** $^{1}$H NMR Spectrum in $CDCl_3$ obtained for a reaction mixture taken after 24 hrs ([Zn($L^H$)]: 1 mol%, TBAB: 10 mol%) showing three peaks of styrene carbonate and three peaks associated to styrene oxide starting material (19% conversion) [* indicates Tetrabutyl ammonium bromide (TBAB) peaks].

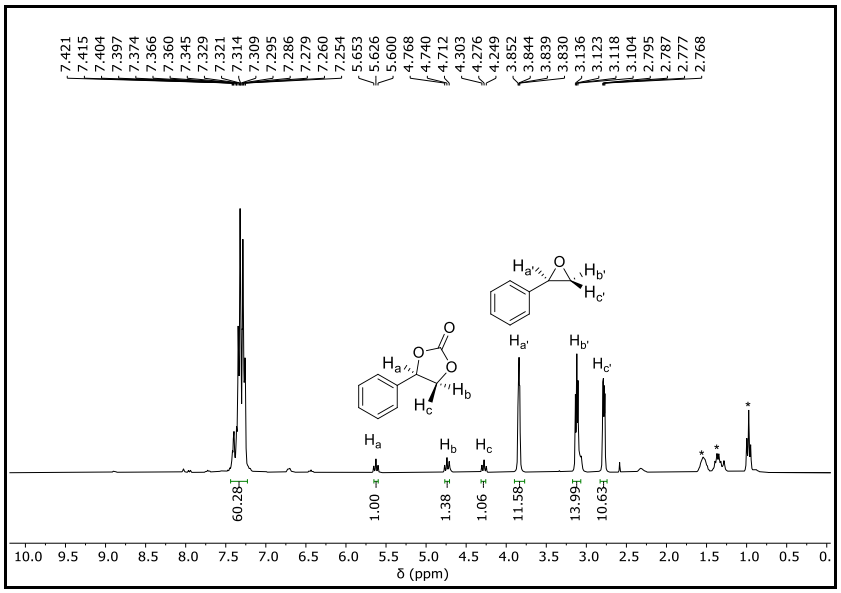

**Figure S56a:** $^{1}$H NMR Spectrum in $CDCl_3$ obtained for a reaction mixture taken after 24 hrs (TBAB: 10 mol%) without catalyst showing three peaks of styrene carbonate and three peaks associated to styrene oxide starting material (7% conversion) [* indicates Tetrabutyl ammonium bromide (TBAB) peaks].

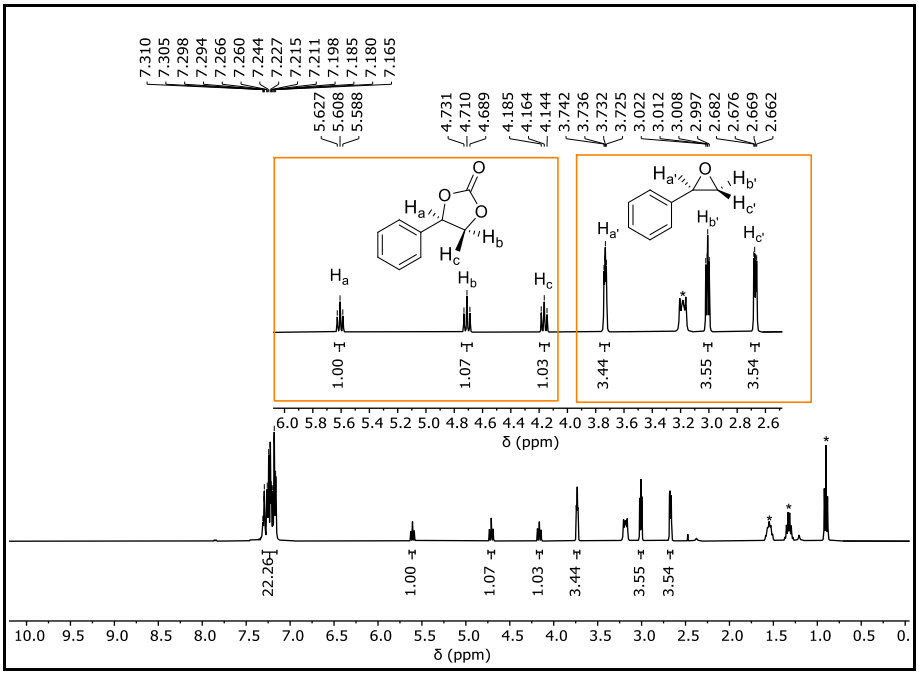


**Figure S57:** $^{1}$H NMR Spectrum in $CDCl_3$ obtained for a reaction mixture taken after 24 hrs ([Zn($L^{H}$)]: 2 mol%, TBAB: 10 mol%) showing three peaks of styrene carbonate and three peaks associated to styrene oxide starting material (23% conversion) [* indicates Tetrabutyl ammonium bromide (TBAB) peaks].

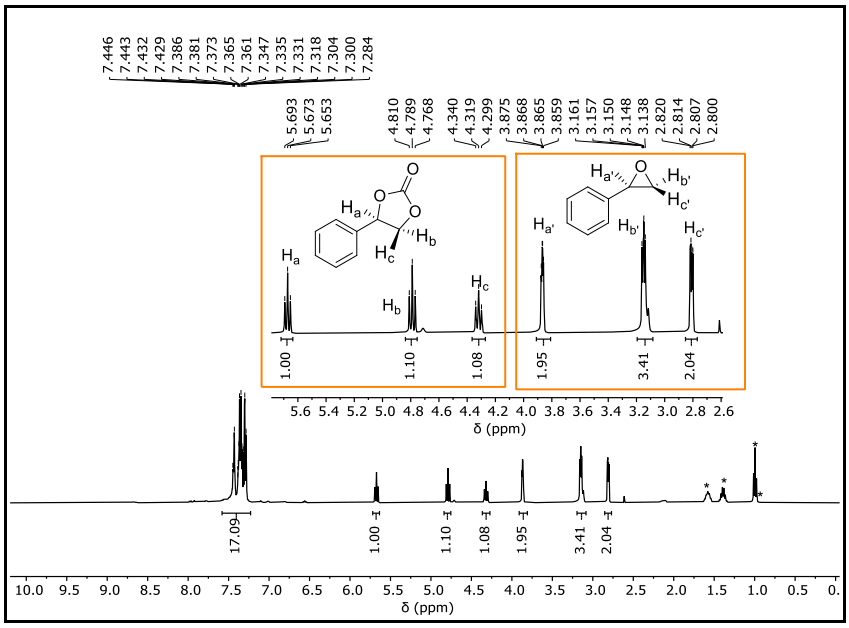


**Figure S57a:** $^{1}H$ NMR Spectrum in $CDCl_3$ obtained for a reaction mixture taken after 24 hrs ([$Zn(L^H)$]: 5 mol%, TBAB: 5 mol%) showing three peaks of styrene carbonate and three peaks associated to styrene oxide starting material (33% conversion) [* indicates Tetrabutyl ammonium bromide (TBAB) peaks].

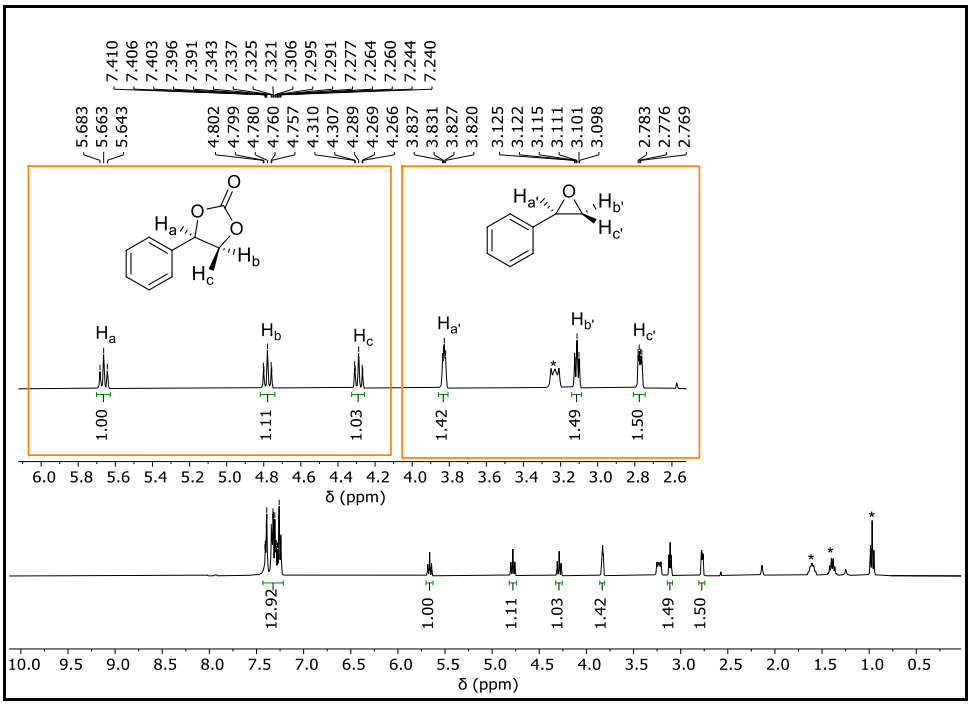


**Figure S58:** $^{1}$H NMR Spectrum in $CDCl_3$ obtained for a reaction mixture taken after 24 hrs ([Zn($L^{H}$)]: 5 mol%, TBAB: 10 mol%) showing three peaks of styrene carbonate and three peaks associated to styrene oxide starting material (41% conversion) [* indicates Tetrabutyl ammonium bromide (TBAB) peaks].

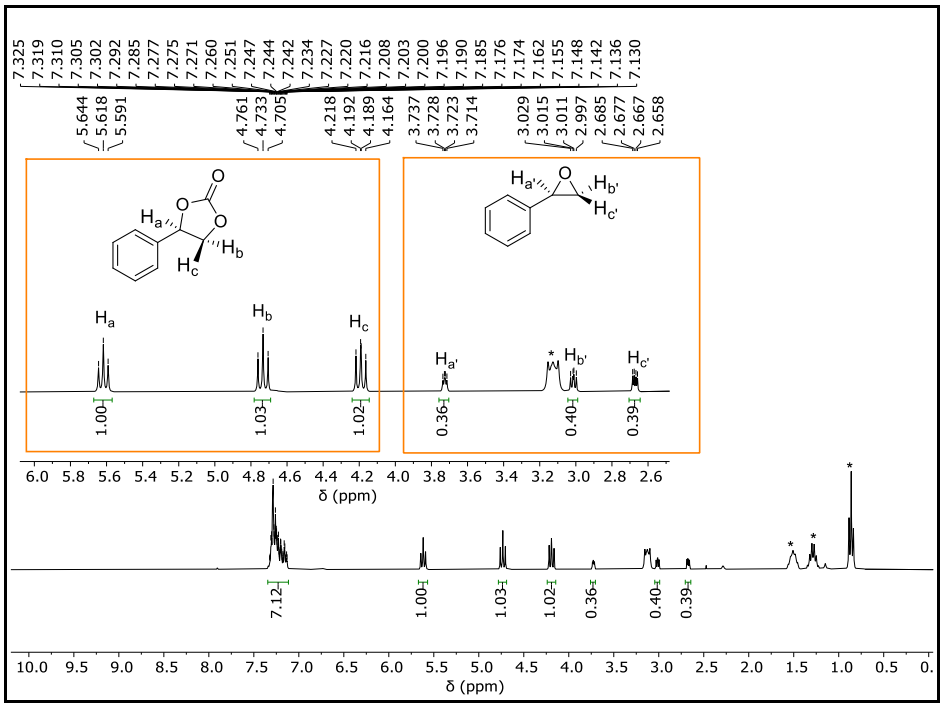


**Figure S59:** $^{1}$H NMR Spectrum in $CDCl_3$ obtained for a reaction mixture taken after 24 hrs ([Zn($L^H$)]: 5 mol%, TBAB: 20 mol%) showing three peaks of styrene carbonate and three peaks associated to styrene oxide starting material (74% conversion) [* indicates Tetrabutyl ammonium bromide (TBAB) peaks].

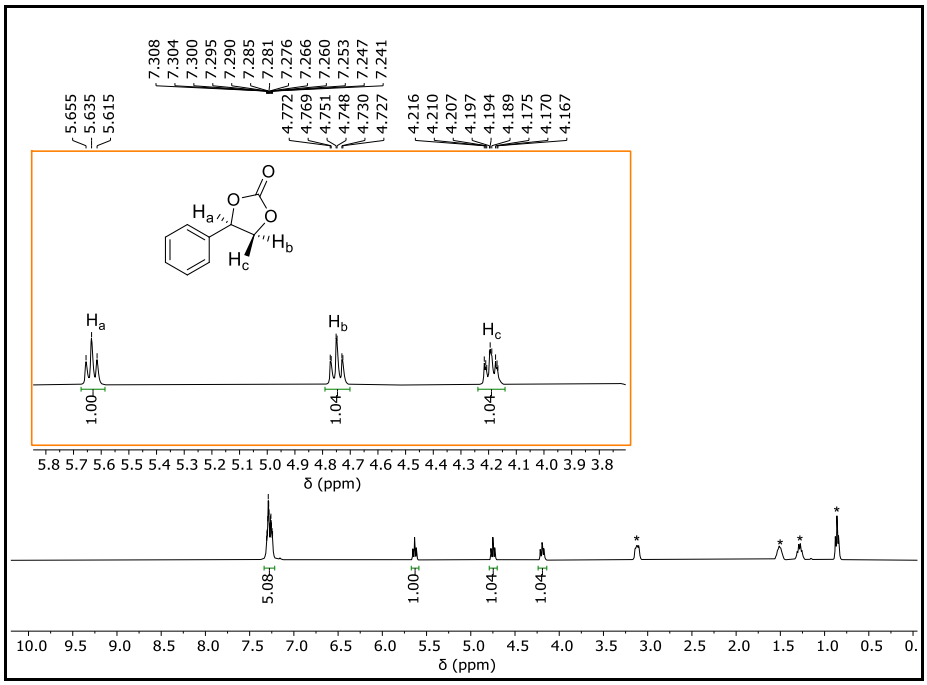


**Figure S60:** $^{1}H$ NMR Spectrum in $CDCl_3$ obtained for a reaction mixture taken after 48 hrs ([Zn($L^{H}$)]: 5 mol%, TBAB: 20 mol%) showing three peaks of styrene carbonate (>99% conversion) [* indicates Tetrabutyl ammonium bromide (TBAB) peaks].

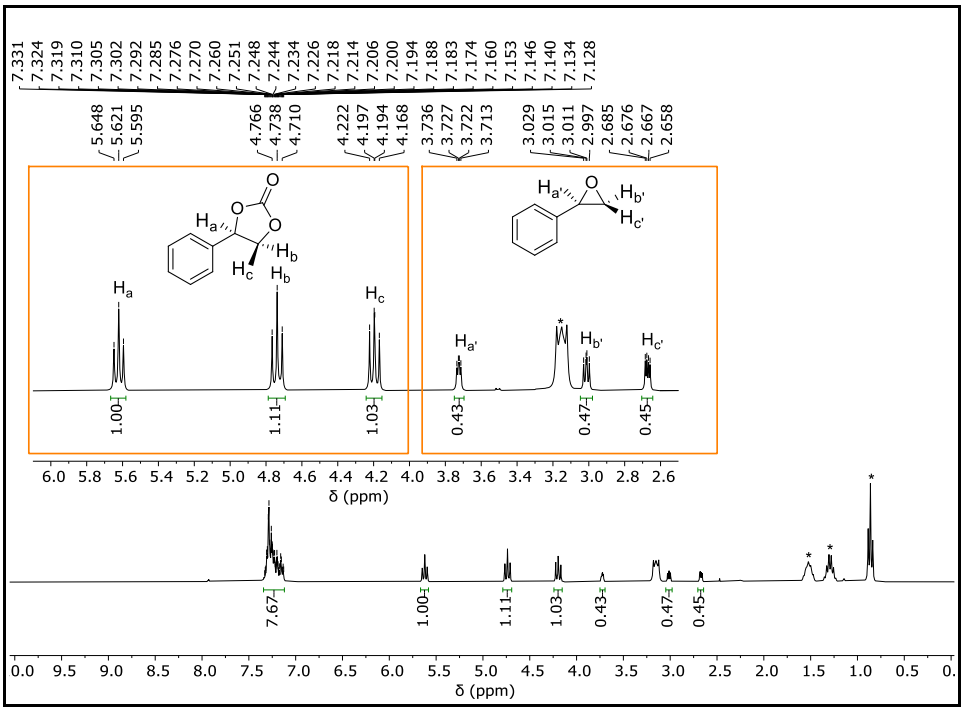


**Figure S61:** $^{1}H$ NMR Spectrum in $CDCl_3$ obtained for a reaction mixture taken after 24 hrs ([$Zn(L^{NO2})$]: 5 mol%, TBAB: 20 mol%) showing three peaks of styrene carbonate and three peaks associated to styrene oxide starting material (70% conversion) [* indicates Tetrabutyl ammonium bromide (TBAB) peaks].

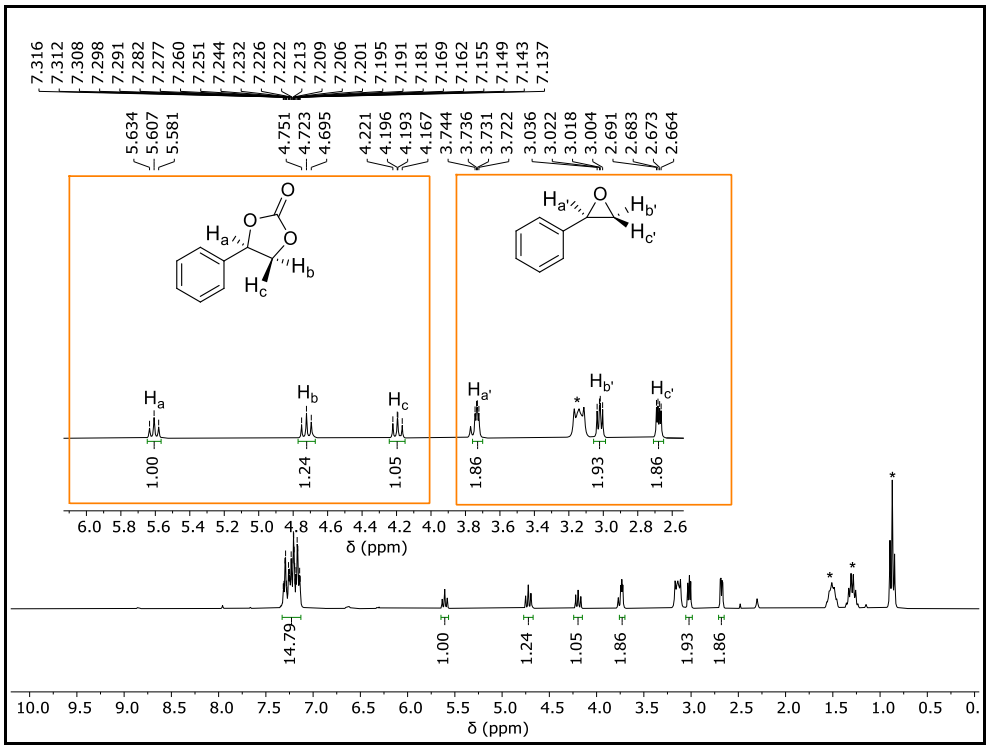


Figure S62: $^{1}H$ NMR Spectrum in $CDCl_3$ obtained for a reaction mixture taken after 24 hrs ([Zn($L^{OMe}$)]: 5 mol%, TBAB: 20 mol%) showing three peaks of styrene carbonate and three peaks associated to styrene oxide starting material (35% conversion) [* indicates Tetrabutyl ammonium bromide (TBAB) peaks].

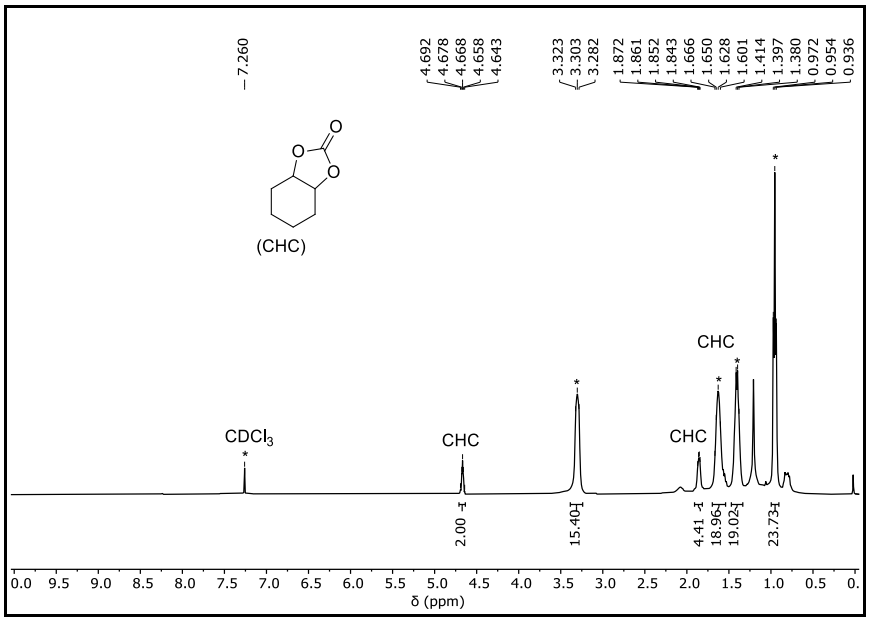


Figure S63: $^{1}H$ NMR Spectrum in $CDCl_3$ obtained for a reaction mixture taken after 24 hrs ([Zn($L^{H}$)]: 5 mol%, TBAB: 20 mol%) showing product peaks of cyclohexane carbonate (CHC) (>99% conversion) [* indicates Tetrabutyl ammonium bromide (TBAB) peaks].

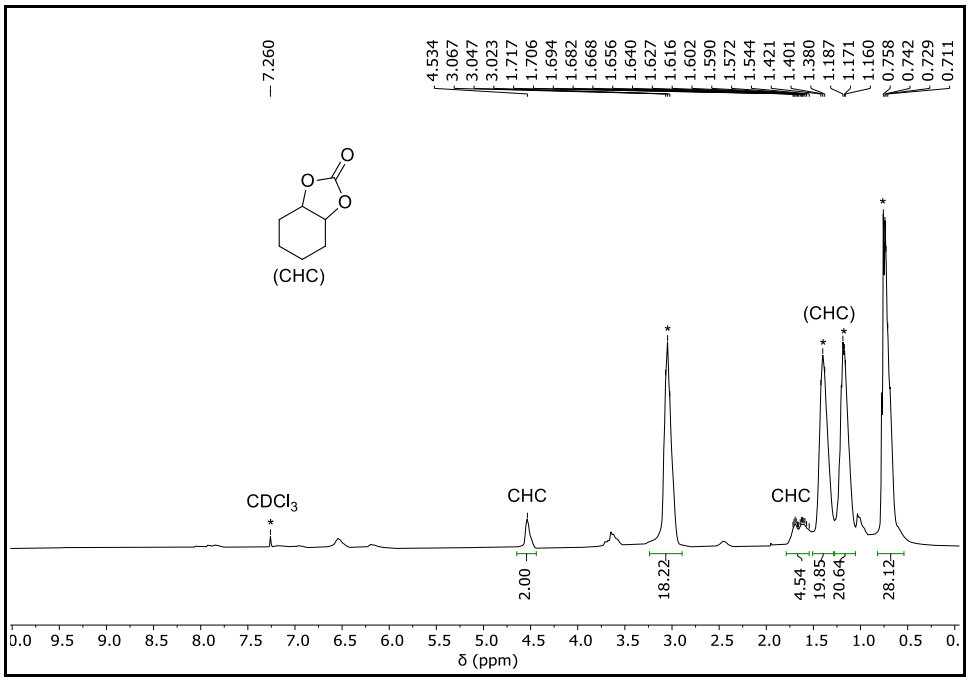

Figure S64: $^{1}H$ NMR Spectrum in $CDCl_3$ obtained for a reaction mixture taken after 24 hrs ([Zn($L^{NO2}$)]: 5 mol%, TBAB: 20 mol%) showing product peaks of cyclohexane carbonate (CHC) (>99% conversion) [* indicates Tetrabutyl ammonium bromide (TBAB) peaks].

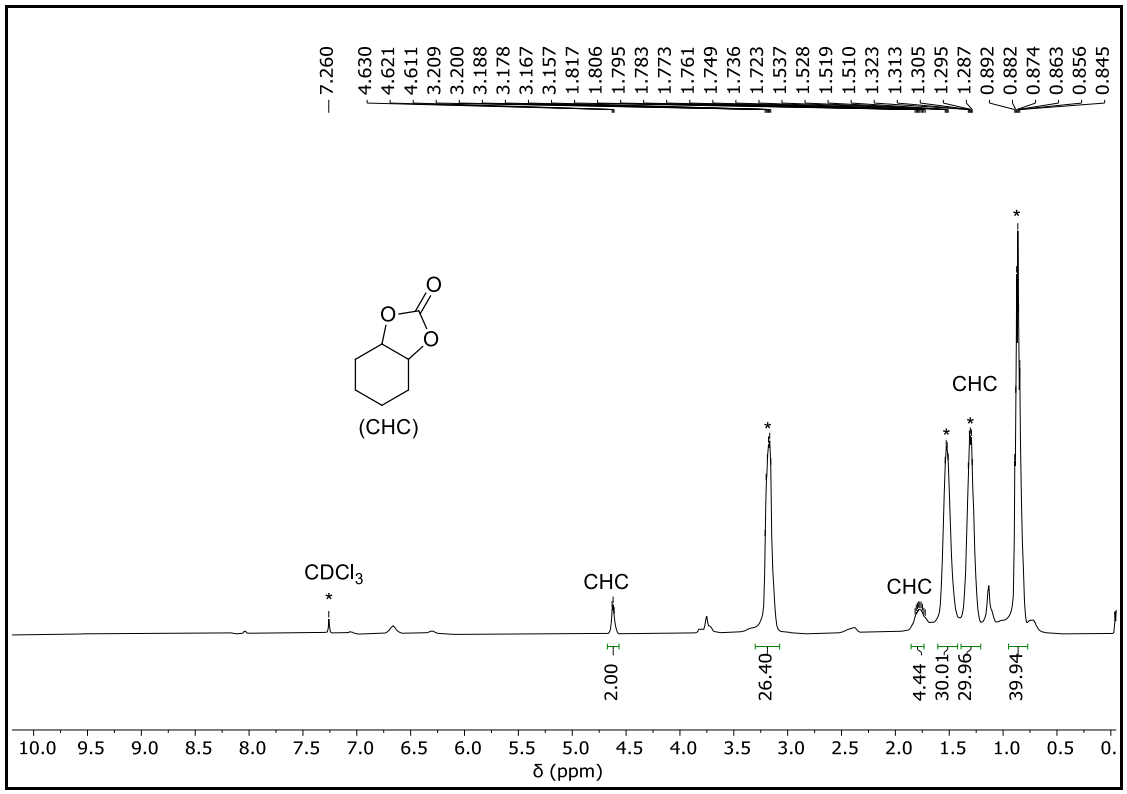


Figure S65: $^{1}H$ NMR Spectrum in $CDCl_3$ obtained for a reaction mixture taken after 24 hrs ([Zn($L^{OMe}$)]: 5 mol%, TBAB: 20 mol%) showing product peaks of cyclohexane carbonate (CHC) (>99% conversion) [* indicates Tetrabutyl ammonium bromide (TBAB) peaks].

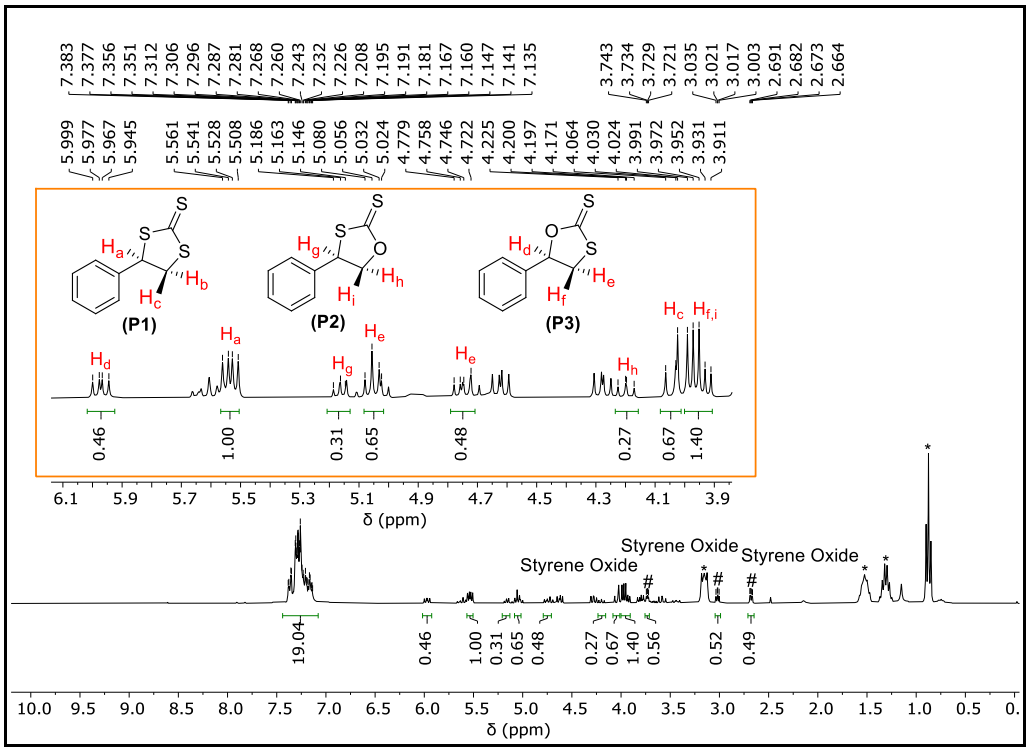


Figure S66: $^{1}H$ NMR in $CDCl_3$ obtained for a reaction mixture taken after 24 hrs ([Zn($L^{H}$)]: 5 mol%, TBAB: 20 mol%, $CS_2$: 0.3 mL) showing three different products and three peaks associated to styrene oxide starting material [* indicates Tetrabutyl ammonium bromide (TBAB) peaks].

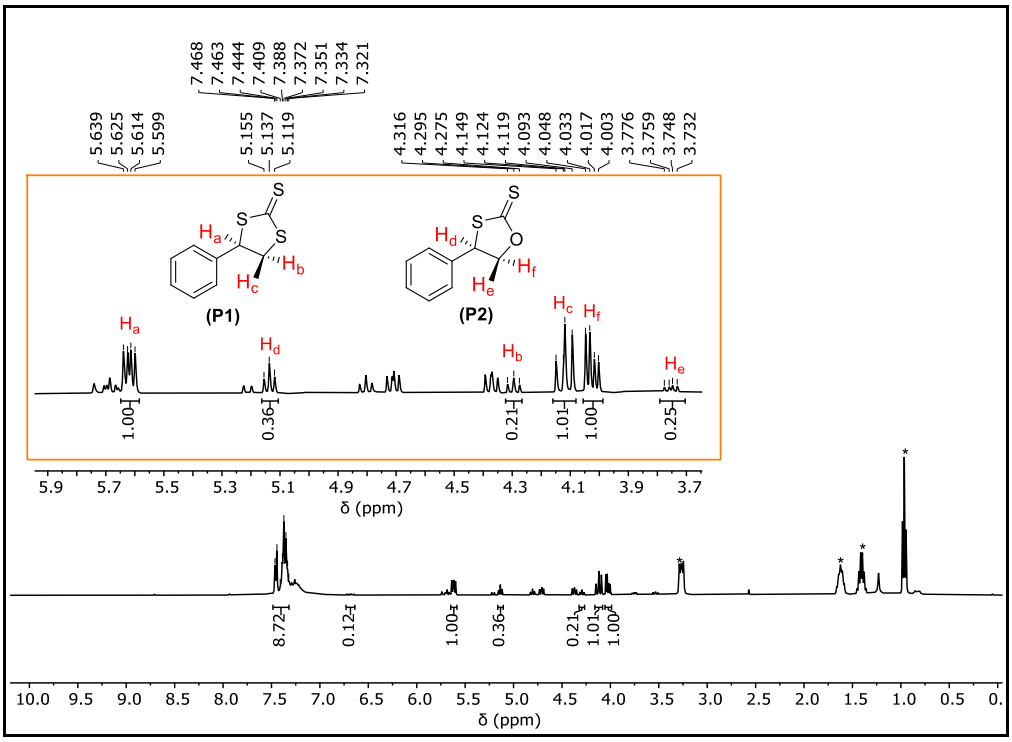


Figure S67: $^{1}H$ NMR in $CDCl_3$ obtained for a reaction mixture taken after 48 hrs ([$Zn(L^{H})$]: 5 mol%, TBAB: 20 mol%, $CS_2$: 0.3 mL) showing two different products [* indicates Tetrabutyl ammonium bromide (TBAB) peaks].

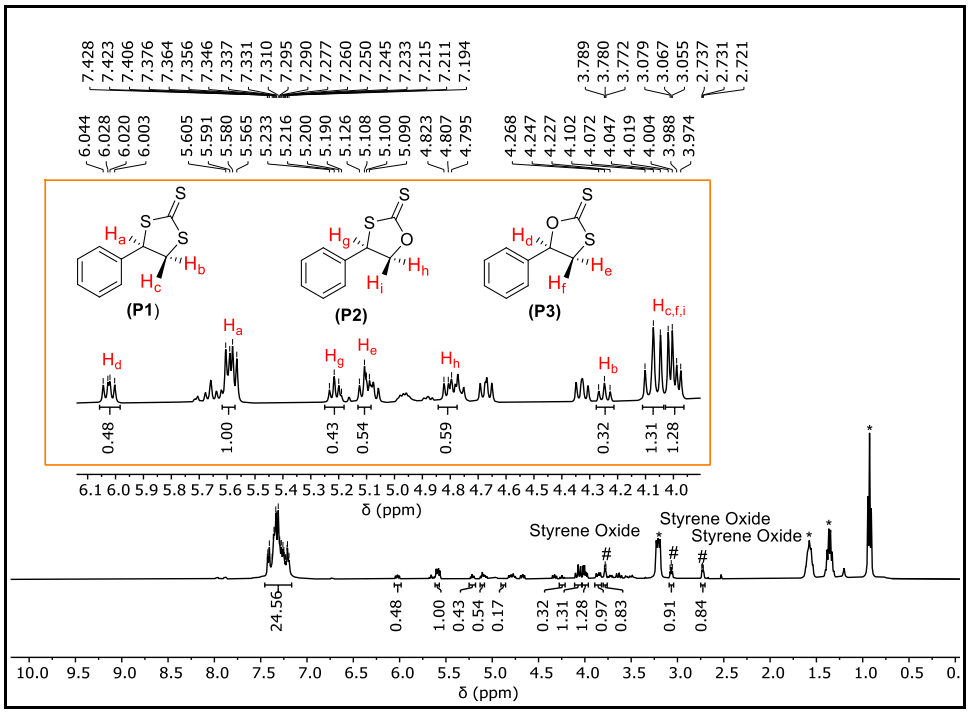


Figure S68: $^{1}H$ NMR in $CDCl_3$ obtained for a reaction mixture taken after 24 hrs ([Zn($L^{NO2}$)]: 5 mol%, TBAB: 20 mol%, $CS_2$: 0.3 mL) showing three different products and three peaks associated to styrene oxide starting material [* indicates Tetrabutyl ammonium bromide (TBAB) peaks].

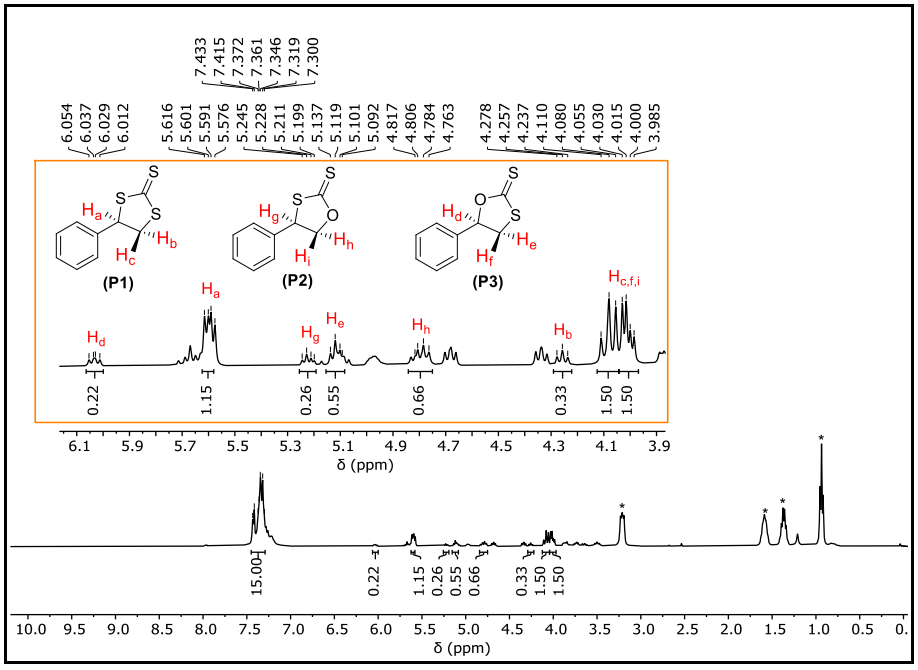

Figure S69: $^{1}H$ NMR in $CDCl_3$ obtained for a reaction mixture taken after 48 hrs ([Zn($L^{NO2}$)]: 5 mol%, TBAB: 20 mol%, $CS_2$: 0.3 mL) showing three different products [* indicates Tetrabutyl ammonium bromide (TBAB) peaks].

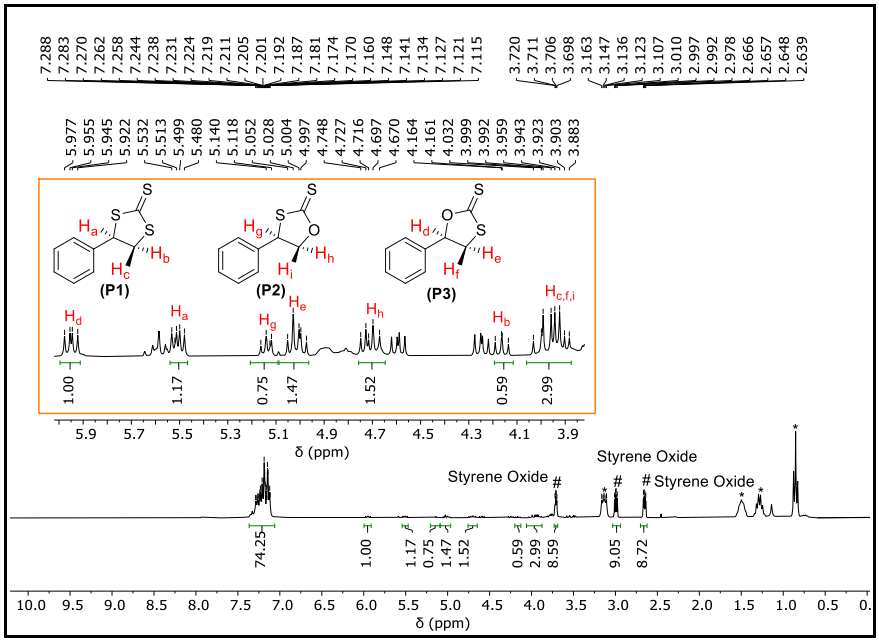


Figure S70: $^{1}H$ NMR in $CDCl_3$ obtained for a reaction mixture taken after 24 hrs ([Zn($L^{OMe}$)]: 5 mol%, TBAB: 20 mol%, $CS_2$: 0.3 mL) showing three different products and three peaks associated to styrene oxide starting material [* indicates Tetrabutyl ammonium bromide (TBAB) peaks].

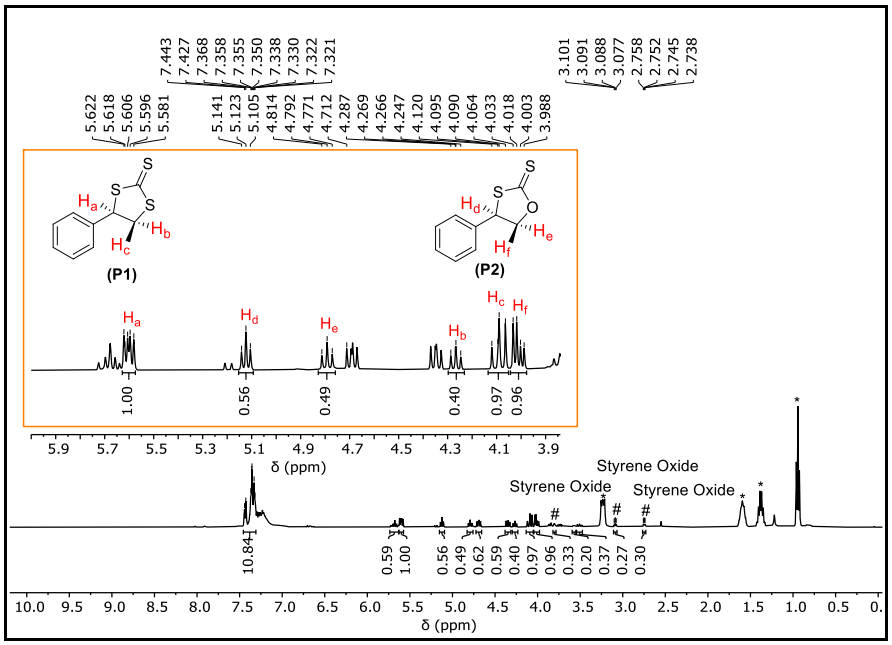


Figure S71: $^{1}$H NMR in $CDCl_3$ obtained for a reaction mixture taken after 48 hrs ([Zn($L^{OMe}$)]: 5 mol%, TBAB: 20 mol%, $CS_2$: 0.3 mL) showing two different products and three peaks associated to styrene oxide starting material [* indicates Tetrabutyl ammonium bromide (TBAB) peaks].

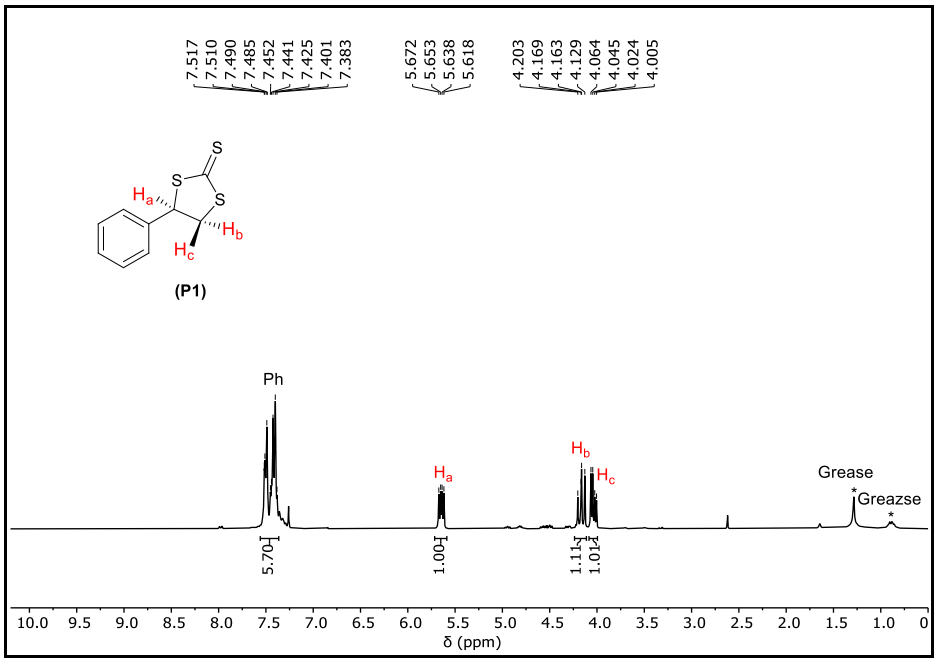

Figure S72: $^{1}$H NMR spectrum of 4-Phenyl-1,3-dithiolane-2-thione in $CDCl_3$.

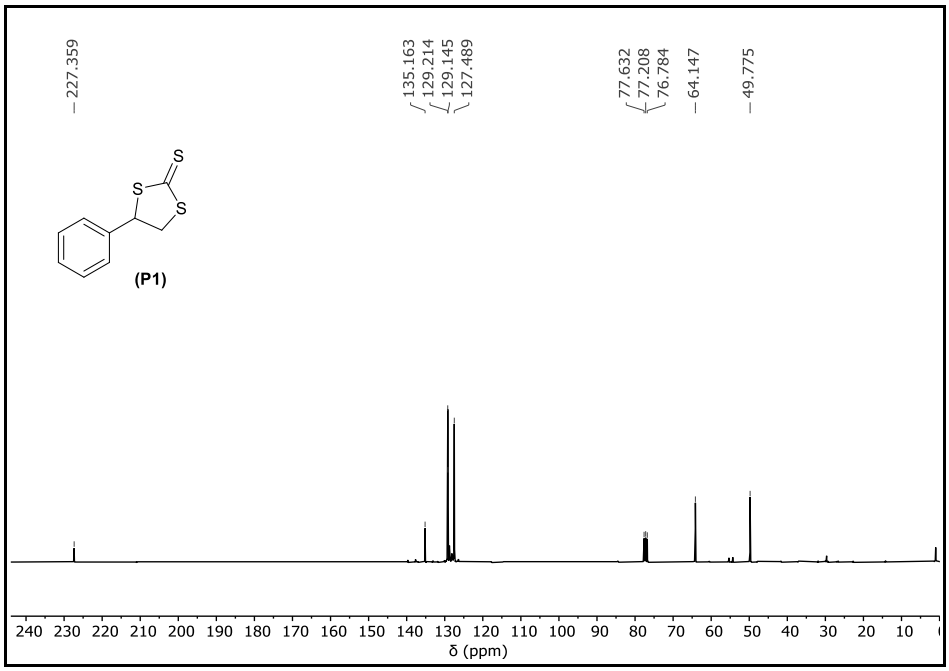


Figure S73: $^{13}$C NMR spectrum of 4-Phenyl-1,3-dithiolane-2-thione in $CDCl_3$.

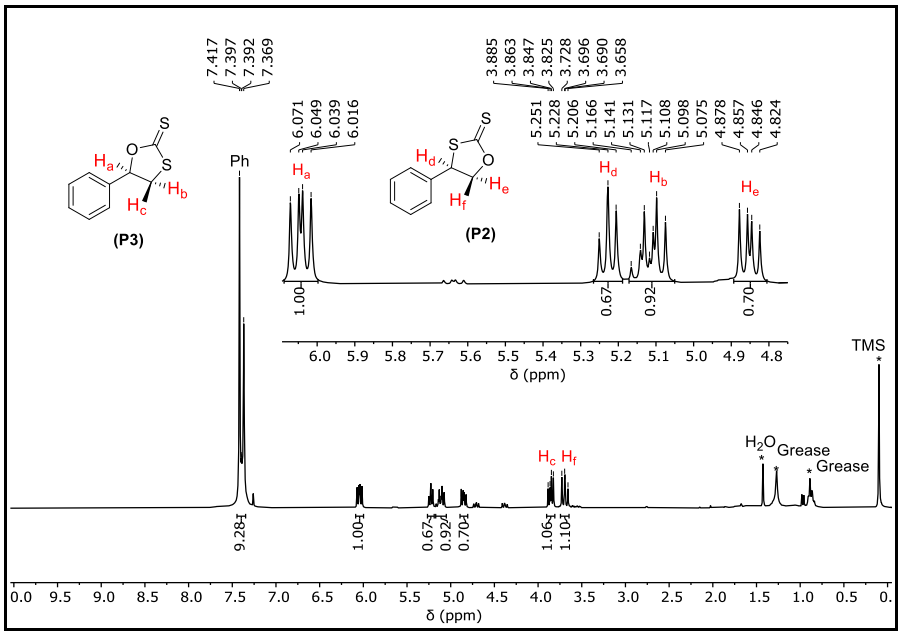

Figure S74: $^{1}H$ NMR spectrum of 5-phenyl-1,3-oxathiolane-2-thione and 4-phenyl-1,3-oxathiolane-2-thione in $CDCl_{3.}$

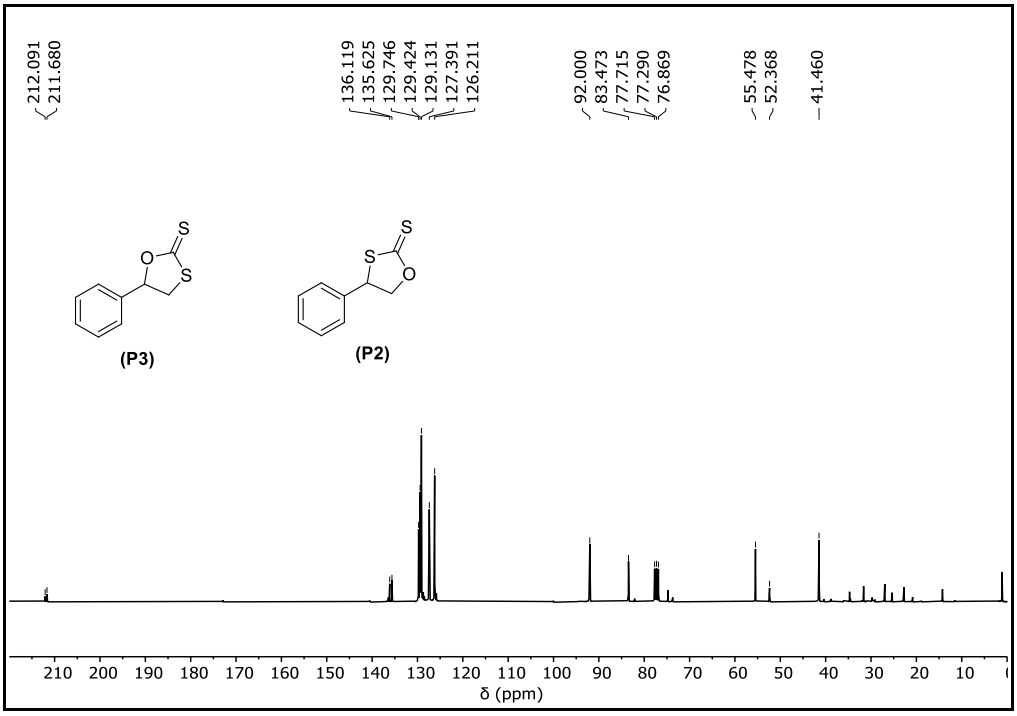


Figure S75: $^{13}C$ NMR spectrum of 5-phenyl-1,3-oxathiolane-2-thione and 4-phenyl-1,3-oxathiolane-2-thione in $CDCl_{3.}$

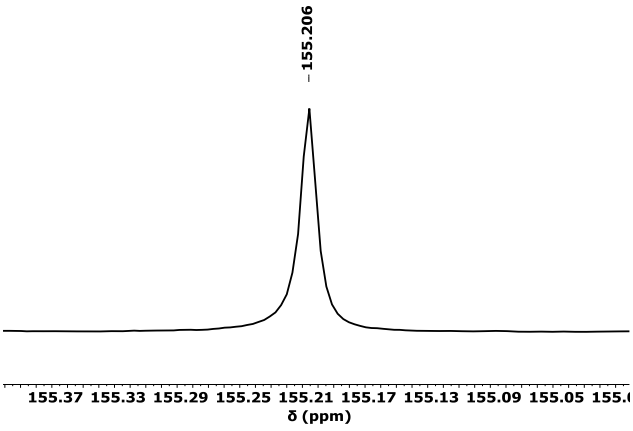


Figure S76: Carbonyl region of $^{13}C$ NMR spectrum of cyclohexane carbonate synthesized using **Zn-1$^{H}$** (Table 5, Reaction 2).

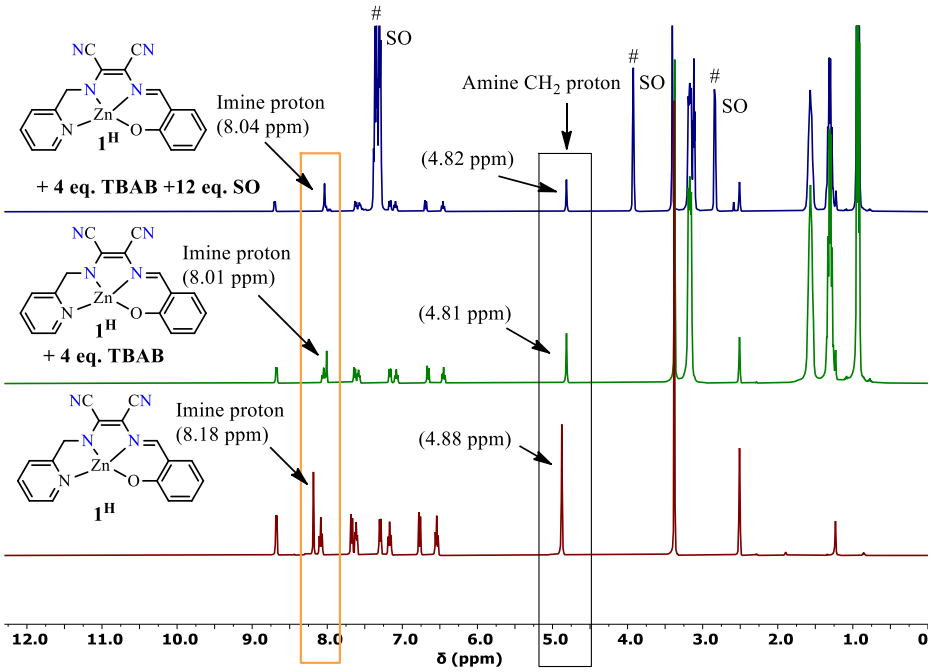


Figure S77: Comparison between the $^{1}$H NMR spectra of complex $\mathbf{1^H}$ (bottom), $\mathbf{1^H}$ in the presence of 4 equiv. TBAB (Middle) and $\mathbf{1^H}$ in the presence of 4 equiv. TBAB and 12 eq. SO (Top) in DMSO-$d_6$ (δH 2.50 ppm).

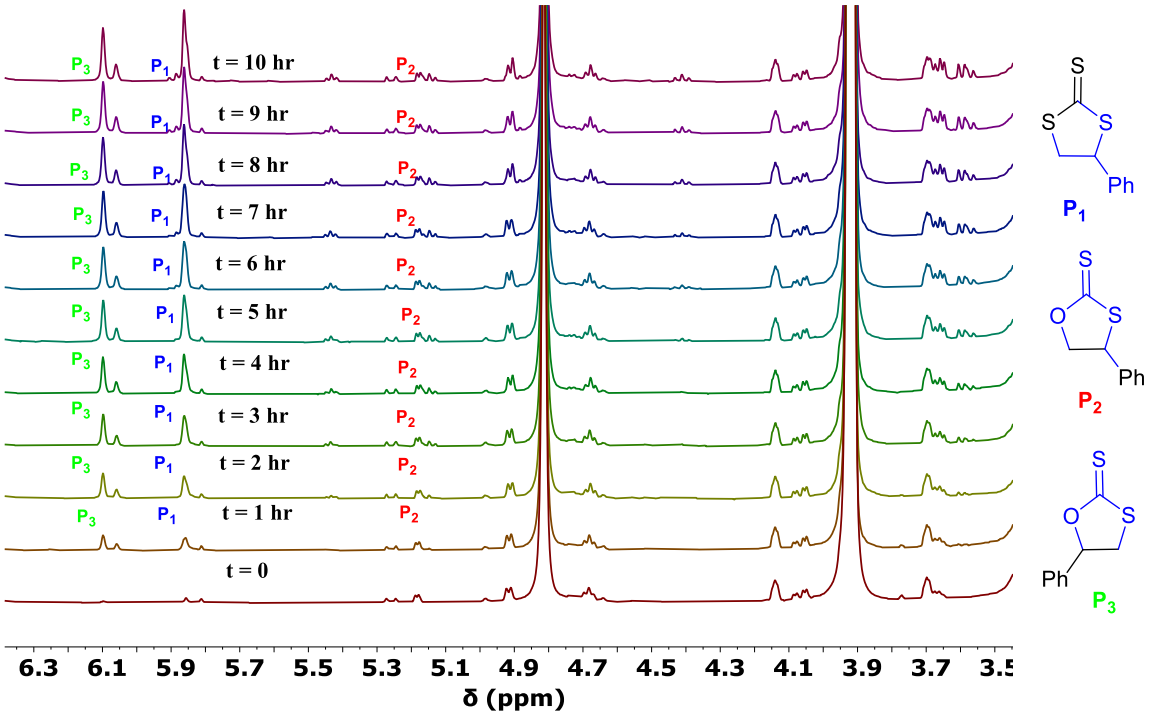

Figure S78: $^{1}$H NMR spectrum of **Zn-1$^{H}$**/TBAB (1:4) added styrene oxide (SO) and $CS_2$ at 22$^{0}$C, NMR taken after 1 h. interval in DMSO-$d_6$.

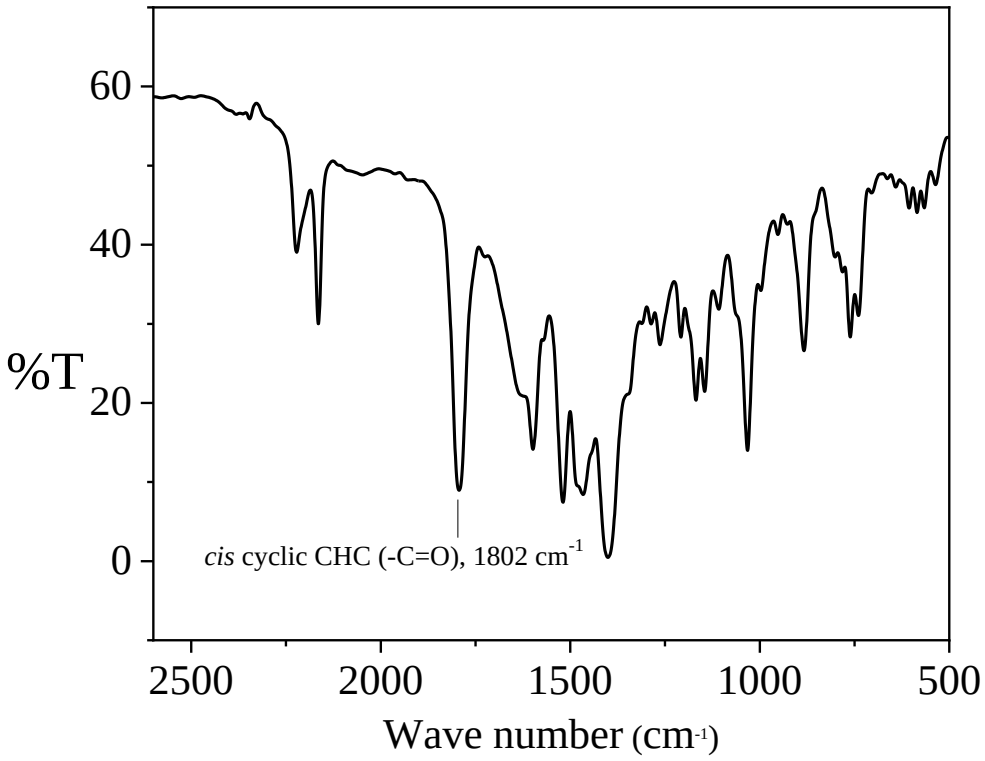


Figure S79: FT-IR spectrum of cyclic cyclohexane carbonate **CHO**(*cis*) synthesized using **Zn-1$^{H}$** as catalyst(Table 5, Reaction 2).

**Table S1: Crystallographic data parameters.**

| Identification code | **$H_2L^{NO2}$** | **$2^{H}$** | **$2^{NO2}$** | **$3^{OMe}$** |
|---|---|---|---|---|
| Empirical formula | $C_{17}H_{12}N_6O_3$ | $C_{20}H_{18}N_6O_2Zn$ | $C_{20}H_{17}N_7O_4Zn$ | $C_{34}H_{49}BrN_6O_2Zn$ |
| Formula weight | 348.33 | 439.77 | 484.77 | 719.07 |
| Temperature/K | 296.15 | 273.15 | 168.24 | 144.99 |
| Crystal system | triclinic | triclinic | monoclinic | triclinic |
| Space group | P-1 | P-1 | $P2_1/n$ | P-1 |
| a/Å | 7.042(3) | 9.322(2) | 11.121(2) | 8.5801(9) |
| b/Å | 9.685(4) | 10.874(3) | 13.472(2) | 11.9385(12) |
| c/Å | 12.244(6) | 11.037(3) | 13.589(3) | 18.0760(17) |
| α/° | 85.324(9) | 109.988(4) | 90 | 91.339(3) |

| | | | | |
|---|---|---|---|---|
| β/° | 81.659(9) | 101.284(4) | 95.903(6) | 97.549(4) |
| γ/° | 84.984(9) | 101.409(4) | 90 | 107.975(3) |
| Volume/$Å^3$ | 821.1(6) | 987.7(4) | 2025.1(6) | 1741.9(3) |
| Z | 1 | 2 | 4 | 2 |
| $\rho_{calc}g/cm^3$ | 1.409 | 1.479 | 1.590 | 1.371 |
| $\mu/mm^{-1}$ | 0.106 | 1.272 | 1.258 | 1.890 |
| F(000) | 360.2 | 452.0 | 992.0 | 752.0 |
| Crystal size/$mm^3$ | 0.1 × 0.09 × 0.07 | 0.22 × 0.15 × 0.11 | 0.2 × 0.18 × 0.1 | 0.25 × 0.15 × 0.11 |
| Radiation | Mo Kα (λ = 0.71073) | MoKα (λ = 0.71073) | MoKα (λ = 0.71073) | MoKα (λ = 0.71073) |
| 2Θ range /° | 3.37 to 50.116 | 4.098 to 54.386 | 4.512 to 50.37 | 5.224 to 69.326 |
| Index ranges | $-8 \le h \le 8$, $-11 \le k \le 11$, $-14 \le l \le 14$ | $-11 \le h \le 11$ $-13 \le k \le 13$ $-14 \le l \le 14$ | $-13 \le h \le 13$ $-16 \le k \le 14$ $-16 \le l \le 16$ | $-13 \le h \le 13$ $-17 \le k \le 18$ $-28 \le l \le 28$ |
| Reflections collected | 14070 | 20163 | 18374 | 26079 |
| Independent reflections | 2879 [Rint = 0.1197, Rsigma = 0.1018] | 4350 [$R_{int}$ = 0.0424, $R_{sigma}$ = 0.0345] | 3598 [$R_{int}$ = 0.0772, $R_{sigma}$ = 0.0590] | 12057 [$R_{int}$ = 0.1085, $R_{sigma}$ = 0.0918] |
| Data/restraints/ parameters | 2879/0/248 | 4350/0/265 | 3598/0/291 | 12057/0/402 |
| Goodness-of-fit on $F^2$ | 1.021 | 1.036 | 1.073 | 1.014 |
| Final R indexes [I>=2σ (I)] | R1 = 0.0628, wR2 = 0.1325 | $R_1$ = 0.0334, $wR_2$ = 0.0778 | $R_1$ = 0.0459 $wR_2$ = 0.1134 | $R_1$ = 0.0510, $wR_2$ = 0.1337 |
| Final R indexes [all data] | R1 = 0.1564, wR2 = 0.1731 | $R_1$ = 0.0466, $wR_2$ = 0.0847 | $R_1$ = 0.0753 $wR_2$ = 0.1388 | $R_1$ = 0.0690, $wR_2$ = 0.1428 |
| Largest diff. peak/ hole / e $Å^{-3}$ | 0.27/-0.32 | 0.61/-0.41 | 0.59/-0.83 | 1.05/-1.12 |

**Table S2: Comparison of cyclic CHC formation by the reaction of CHO and $CO_2$ using Zn complex as a catalyst**

| **Entry** | **Zn Catalyst (mol%)** | **Co-catalyst (mol%)** | **Condition** | **Yield % (Cyclic CHC)** | **Reference (suggested by reviewer) (I.F=Impact Factor)** | **Remark** |
|---|---|---|---|---|---|---|
| 1. | 5 | TBAB (5) | T = $50^0$C, time = 24 h, $P_{CO2}$ = 10 bar | 90 | Dalton Trans., 2019, 48, 10733–10742. (I.F=4.569) | High P and High Yield |
| 2. | 0.1 | None | T = $120^0$C, time = 32 h, $P_{CO2}$ = 1.7 MPa | 90 | Chem. – Eur. J., 2016, 22, 6556–6563. (I.F=5.02) | High T and high P and High Yield |
| 3. | 0.5 | TBAB (0.5) | T = $70^0$C, time = 18 h, $P_{CO2}$ = 10 bar | 93 | Dalton Trans., 2023, 52, 6105-6116. (I.F=4.569) | High P and High Yield |
| 4. | 0.5 wt% of CHO | None | T = $100^0$C, time = 4 h, $P_{CO2}$ = 3 | 17 | Dalton Trans., 2020, 49, 312-321. | High T and High P, poor |

| | | | | | | |
|---|---|---|---|---|---|---|
| | | | MPa | | (I.F=4.569) | yield |
| 5. | 0.14 | TBAB (0.2) | T = 80$^0$C, time = 24 h, $P_{CO2}$ = 50 bar | 27 (cis : trans = 9:1) | J. $CO_2$ Util., 2016, 14, 10–22. (I.F=8.321) | High T and high P. poor yield |
| 6. | 1 | TBAI (1) | T = 100$^0$C, time = 12 h, $P_{CO2}$ = 5 MPa | 34 | Green Chem., 2016, 18, 226–231. (I.F=11.034) | High T and high P. poor yield |
| 7. | 0.04 | TBAB (0.4) | T = 100$^0$C, time = 3 h, $P_{CO2}$ = 30 bar | 27 | Polyhedron, 2019, 173, 114134. | High T and high P. poor yield |
| 8. | 0.3 | TBAB (0.6) | T = 100$^0$C, time = 16 h, $P_{CO2}$ = 0.1 MPa | 14 | **J**. Mol. Catal. A: Chem., 2016, 420, 208–215. (I.F=5.089) | High T, poor yield |
| 9. | 0.13 | TBAB (0.2) | T = 80$^0$C, time = 3 h, $P_{CO2}$ = 20 bar | 28 | Molecular Catalysis, 2023, 538, 112992. (I.F=5.089) | High T and high P. poor yield |
| 10. | 0.2 | TBAB (0.2) | T = 80$^0$C, time = 20 h, $P_{CO2}$ = 50 bar | 10 | **J**. Mol. Catal. A: Chem., 2015, 400, 104-110. (I.F=5.089) | High P. poor yield |
| **11.** | **5** | **TBAB (20)** | **T = 70$^0$C, time = 24 h, $P_{CO2}$ = 1 bar** | **>99** | **Present work** | **-** |

**Table S3: Important references related to the selective cyclic carbonate formation by the reaction of $CO_2$ cycloaddition to epoxide.**

| **Entry** | **Zn Catalyst (mol%)** | **Co-catalyst (mol%)** | **Condition** | **Yield %** | **TOF ($h^{-1}$)** | **Reference (suggested by reviewer) (I.F=Impact Factor)** |
|---|---|---|---|---|---|---|
| 1. | 0.1 | None | T = 120$^0$C, time = 32 h, $P_{CO2}$ = 1.7 MPa | 90 (Cyclic CHC) | - | Chem. – Eur. J., 2016, 22, 6556–6563. (I.F=5.02) |
| 2. | 0.5 | TBAI (2) | T = 100$^0$C, time = 24 h, $P_{CO2}$ = 1 bar | 76 (Cyclic CHC) | 6.12 | Catalysis Today, 2021, 375, 324-33. (I.F=6.562) |
| 3. | 2 (Hydrogen Bond Donor) | TBAB (4) | T = RT, time = 23 h, $P_{CO2}$ = 1 bar | 35(Epichlorohydrin = ECH) | 1.89 | Advanced Synthesis & Catalysis, 2019, 361, 366-373. |
| 4. | 0.2 (cata = $ZnCl_2$) | TBAI (0.8) | T = RT, time = 24 h, $P_{CO2}$ = 1 bar | 27 (SO) | 6 | Chem. Ber. 1986, 119, 1090– 1094. |

| | | | | | | |
|---|---|---|---|---|---|---|
| **5.** | **5** | **TBAB (20)** | **T = 70$^0$C, time = 24 h, $P_{CO2}$ = 1 bar** | **>99 (Cyclic CHC)** | **0.83** | **Present work** |

**Table S4: Important references related to the selective cyclic thio-carbonate formation by the reaction of $CS_2$ cycloaddition to epoxide.**

| Catalyst | Substrate | Product | Yield (%) | Selectivity (%) | Condition | Reference |
|---|---|---|---|---|---|---|
| DBU | $CS_2$+Different epoxides | Cyclic + polymer+ COS | 3.8 | | T= 120 °C, Time= 12h | Macromolecules, **2020**, *53*, 1, 233–239. |
| TBD | | | 4.4 | | | |
| DBN | | | 3.2 | | | |
| MTBD | | | 3.7 | | | |
| DMAP | | | 0 | | | |
| | | | | | | |
| Hollow $CoAl_2O_4$ | SO+$CS_2$ | Cyclic | 20 | | T= 25$^0$C, Time= 3h | Journal of the Taiwan Institute of Chemical Engineers, **2020**, 1-13. |
| | | | 50 | | T= 50$^0$C, Time= 3h | |
| | | | 85 | | T= 70$^0$C, Time= 3h | |
| | | | 96 | | T= 90$^0$C, Time= 3h | |
| | | | | | | |
| N-heterocyclic carbene/LiCl(Br) | $^n$BuO+$CS_2$ | 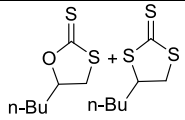 | | 60:23 | T= 40$^0$C, Time= 24 h. | Tetrahedron, **2017**, *73*, 5706e5714. |
| | | | | 46:0 | | |
| | | | | 88:8 | | |
| | | | | | | |
| $Me_2N$-$C_3H_6$-MS-1 | EtO+$CS_2$ | Four different cyclic products 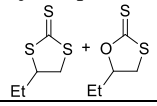 | 99 | 18:80 | T= 100 °C, Time= 6 h | Ind. Eng. Chem. Res., **2018**, *57*, 3, 891–896. |
| | | | | | | |
| LiO$^t$Bu | $CS_2$+Different epoxides | 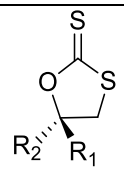 ( 17 entries) | 80-90 | | T= 25 °C, Time= 5 h, solvent free | Org. Biomol. Chem., **2016**, *14*, 7480–7489. |
| | | | | | | |
| $[HO(CH_2)_2PBu_3]I$ | EtO+$CS_2$ | 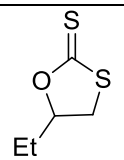 | 11 | 0 | T= RT, Time= 5 h | ChemCatChem, **2016**, *8*, 2027 – 2030. |
| LiBr | | | 21 | 76 | | |
| LiO$^t$Bu, LiBr | | | 99 | 81 | | |
| LiO$^t$Bu | | | 99 | 78 | | |

| | | | | | | |
|---|---|---|---|---|---|---|
| | | | | | | |
| Asymmetric bis-Schiff-base **Zn(II) complex** | CHO+ $CS_2$ | Polymer+ Cyclic | 83 | | T= $80^0$C, Time= 8 h | Inorganic Chemistry Communications, **2015**, *55*, 132–134. |
| | | | 20 | | | |
| | | | 17 | | | |
| | | | 2 | | | |
| | | | 47 | | | |
| | | | 40 | | | |
| | | | | | | |
| Potassium ethyl xanthogenate : Epoxide (1:1) | CHO+$CS_2$ | 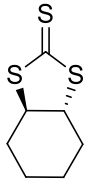 | 100 | | T= $35^0$C, Time= 12h, EtOH | ARKIVOC, **2014** , 16-41. |
| | | | 100 | | T= $35^0$C, Time= 12h, MeOH | |
| | | | | | | |
| Binary Lewis acid– Lewis base catalyst | $CS_2$+Different epoxides | Three different products | 11 | | T= $60^0$C, Time= 12h | Appl. Organomet. Chem., **2012**, *26*, 614–618. |
| | | | 22 | | T= $60^0$C, Time= 10h | |
| | | | | | | |
| Bimetallic Aluminum(salen) Complex (5 mol%) | **PO+$CS_2$** | 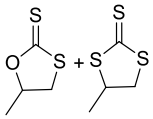 | 95 | 5:95 | T= $90^0$C, Time= 16 h | J. Org. Chem., **2010**, *75*, 6201–6207. |
| | | | 59 | 71:29 | | |
| | | | | | | |
| Aluminium(salen) catalyst | **PO+$CS_2$** | 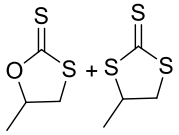 | 95 | | T= $90^0$C, Time= 16h | Synlett, **2010**, No. 4, 623–627 |
| | | | | | | |
| Ti catalyst | | 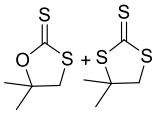 | 100 | | T= $90^0$C, Time= 24 h | ChemCatChem, **2014**, *6*, 1252-1259. |
| | | | | | | |
| (Salen)CrCl | CHO+$CS_2$ | 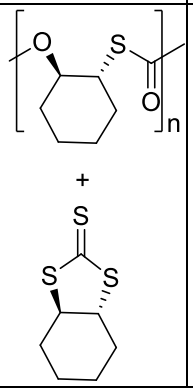 | 40.6 | | T= $40^0$C, Time= 4h | Dalton Trans., **2009**, 8891–8899. |

| | | | | | | |
|---|---|---|---|---|---|---|
| | | | 61.4 | | T= $50^0$C, Time= 4h | |
| | | | 67.7 | | T= $60^0$C, Time= 4h | |
| | | | | | | |
| Zn-$Co^{III}$ DMCC | $PO+CS_2$ | Polymer | 94.6 | | T= $100^0$C, Time= 6h | Macromolecules, **2008,** *41*, 1587-1590. |
| | | | | | | |
| Hydrotalcite MG30 (Heterogeneous catalysis) | $SO+CS_2$ | 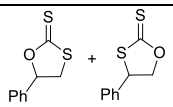 | 83 | 62:38 | T= $50^0$C, Time= 5h | **SYNTHESIS, 2008**, *1*, 0053–0056. |
| Hydrotalcite MG30 | | 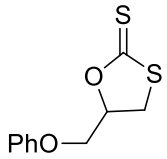 | 84 | 99 | T= $50^0$C, Time= 3h | |
| Hydrotalcite MG70 | | | 67 | 98 | | |
| Alumina | | | 21 | 98 | | |
| MgO | | | 16 | 99 | | |
| MgO/alumina (30:70) | | | 33 | 98 | | |
| Hydrotalcite MG30 | | **No reaction** | | | **Room temp** | |
| Hydrotalcite MG30 | $SO+CS_2$ | 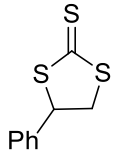 | | | T= $100^0$C, Time= 5h | |
| | | | | | | |
| NaH (10 mol%) | $SO+CS_2$ | 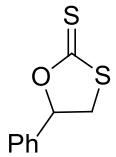 | 95 | | MeOH | SYNLETT, **2008**, *6*, 0889–0891. |
| NaOH (10 mol%) | | 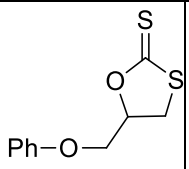 | 95 | | MeOH | |
| | | | | | | |
| Ti catalyst | $PO+CS_2$ | 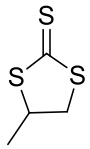 | Quant ative | | T= $120^0$C, Time= 48h | Tetrahedron, **2001,** *57*, 7149-7152. |
| | | | | | | |
| $Et_3N$ | | 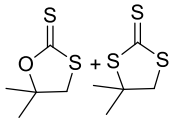 | 4 | | T= $100^0$C, Time= 20h $CS_2$= 0.1 MPa | Bull. Chem. Soc. Jpn., **1988**, *61*, 921-925. |
| $Et_3N$ | | | 76 | 68:8 | T= $100^0$C, | |

| | | | | | | |
|---|---|---|---|---|---|---|
| | | | | | Time= 20h<br>$CS_2$= 800 MPa | |
| N,N-Dimethylethylamine | | 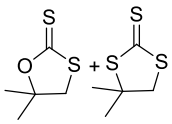 | 85 | 67:18 | T= $100^0$C,<br>Time= 20h<br>$CS_2$= 800MPa | |
| Pyridine | | 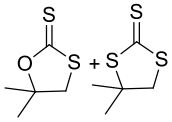 | 92 | 88:4 | T= $100^0$C,<br>Time= 20h<br>$CS_2$= 800 MPa | |
| | | | | | | |
| NaI | | Five different products | 66 | | T= RT,<br>Time = 24h | J. Org. Chem., **1996**, *60*, 473-475. |
| LiI | | | 75 | | T= RT,<br>Time = 2h | |
| LiBr | | | 71 | | | |
| LiCl | | | 53 | | | |
| | | | | | | |
| **Diethylzinc-Electron-Donor Catalyst** | PO+$CS_2$ | Polymer | 7.5 | | T= $25^0$C,<br>Time = 26.5h | JOURNAL OF POLYMER SCIENCE, **1977,** *15*, 937-944. |

**Note on the Crystal structure analysis for $H_2L^{NO2}$:**

Although, the structure of this ligand molecule is quite flexible compare to metal complexes. Because of that it was always difficult to obtain a good quality crystal. However, after several attempts, fortunately a suitable crystal for x-ray diffraction was obtained. After analyzing the image spot intensity, we have chosen an exposure of 10 seconds with a scan width of 2 degree where both of image below explain the resolution.